MASTER THESIS

EVALUATING THE FEASIBILITY AND EFFECTS OF VIBROTACTILE PLANTAR PRESSURE FEEDBACK ON POSTURAL BALANCE IN INDIVIDUALS WITH BILATERAL LOWER EXTREMITY AMPUTATION: A PILOT STUDY DESIGN

Monique de Waal - Liklikuwata

FACULTY OF ENGINEERING TECHNOLOGY
DEPARTMENT OF BIOMECHANICAL ENGINEERING

EXAMINATION COMMITTEE
Prof.dr.ir. Herman van der Kooij, UT
Dr. Erik C. Prinsen, UT
Dr. Mhairi K. MacLean, UT
Dr. Maarten R. Prins, MRC
Niels Jonkergouw MSc, MRC

UNIVERSITY OF TWENTE.

MRC Aardenburg

2025-07

ABSTRACT

Individuals with bilateral lower extremity amputation face significant challenges in maintaining postural stability due to the absence of proprioceptive and plantar pressure feedback, leading to increased fall risk. While vibrotactile feedback systems have shown promise in improving gait, their impact on static postural balance remains unexplored. This pilot study investigated the feasibility and preliminary effects of the Suralis system, a commercially available solution providing gait-synchronized vibrotactile sensory feedback. Within this study, it served as a tool for both measuring postural balance and delivering plantar pressure feedback during four postural balance tasks to individuals with bilateral lower extremity amputation.

To validate the Suralis system's measurement capabilities, we conducted analyses including pressure-force comparisons, pressure distribution heatmaps, and vibration motor activation analysis. A custom multiple linear regression (MLR) model was employed to estimate the centre of pressure (CoP) from Suralis sensor readings, validated against force plates (GRAIL system). The study design involved an ABAB introduction/withdrawal protocol across four standing tasks (eyes open, eyes closed, cognitive dual task, reach and target task) to assess the intervention's effect on centre of pressure speed (CoPs) and Margin of Stability (MoS).

Our findings indicate that the Suralis system, in its current state, demonstrates limitations in delivering consistent vibrotactile feedback, with inconsistencies observed in vibration motor activation based on individual sensor thresholds. However, the system shows accurate measurement capabilities for postural balance. The MLR model estimates the CoP with a Root Mean Squared Error (RMSE) below 10 mm. Due to participant discomfort leading to early study termination, the limited baseline data from a single participant did not allow for conclusive evaluation of the intervention's effects on postural balance.

Abbreviations and definitions:

Abbreviation	*Full term*	*Definition*
AP	*Anteroposterior*	Relating to or directed along the front-to-back axis of the body
ML	*Mediolateral*	Relating to or directed along the side-to-side axis of the body
CoP	*Centre of Pressure*	The point of application of the ground reaction force on the support surface
CoPs	*Centre of Pressure speed*	The velocity of the CoP
BoS	*Base of Support*	The Area enclosed by the points of contact between the body and the ground
CoM	*Centre of Mass*	The average position of the body its mass
xCoM	*Extrapolated Centre of Mass*	A projection of the velocity adjusted CoM location on the support surface
MoS	*Margin of Stability*	The shortest distance between the xCoM and the edge of the BoS
GRAIL	*Gait Real-time Analysis Interactive Lab*	A real-time analysis lab by Motek Medical BV that collects biomechanical data, further explained in section 2.2.
MoCap	*Motion Capture*	A system used for recording movement
RMSE	*Root Mean Squared Error*	A measure of the differences between values predicted by a model or estimator and the values observed
MLR	*Multiple Linear Regression*	A statistical technique that uses several explanatory variables to predict the outcome of a response variable
EO	*Eyes Open*	A condition where participants perform a task with their eyes open
EC	*Eyes Closed*	A condition where participants perform a task with their eyes closed
CT	*Cognitive Task*	A task designed to engage mental processes such as attention
RTT	*Reach and Target Task*	A motor task involving reaching to a specific target

TABLE OF CONTENTS

1. INTRODUCTION

Individuals with bilateral lower extremity amputation face unique challenges in maintaining postural stability due to the absence of sensory feedback from their lower limbs, particularly the lack of proprioception and plantar pressure sensation [1-5]. Unlike individuals with intact limbs, they cannot rely on the ankle strategy to stabilize themselves against balance disturbances [2, 6, 7]. The lack of sensory feedback and ankle strategy leads to a greater dependence on compensatory strategies, such as increased upper body and hip compensations. As a result, individuals with bilateral lower limb amputation experience increased postural sway, particularly in the anteroposterior (AP) direction compared to the mediolateral (ML) direction. This significant gap in postural stability profoundly contributes to their higher risk of falls and increased energy consumption compared to healthy individuals [1, 6, 8].

Several approaches have been explored to restore sensory input in people with amputation using non-invasive methods. Wentink et al. investigated both electrotactile and vibrotactile feedback systems, applying them to the upper leg. Their research showed that vibrotactile feedback was not only well perceived but also usable for conveying spatial information in a consistent and interpretable way [9]. In a follow-up study, it was explored if integrating such feedback into upper leg prostheses could improve intuitive user control and enable more natural, automatic responses between user and device [10].

More recently, Kalff et al. evaluated the Suralis system among individuals with lower extremity amputation. The Suralis provides gait-synchronized vibrotactile feedback from a pressure-sensing sock to an actuator cuff worn on the thigh. In a prospective study, participants used the system at home for over 60 days, and clinically meaningful improvements in gait speed, stability, and coordination were observed. Significant improvements were reported in Timed Up and Go (TUG) tests, as well as clinically meaningful trends in walking speed, though effects on standing balance were not investigated [11]. Similarly, Valette et al. also investigated a system (OmniFeel) that utilizes the same pressure-sensing insole, though with different vibrotactile actuators, for intuitive feedback during dynamic tasks like walking and stair ambulation [12].

While these studies demonstrate the feasibility and user acceptance of vibrotactile feedback systems in individuals with lower limb amputation, they have primarily focused on the effects of dynamic tasks such as walking. As a result, the potential benefits of plantar pressure feedback for improving static postural balance remains unexplored. Specifically, there is a lack of evidence on whether such feedback can reduce postural sway or enhance stability during quiet standing in individuals with lower extremity amputation.

In parallel, strategies for addressing sensory deficits in other patient groups may offer transferable insights for individuals with amputation. For example, Ariës et al. [13] reviewed somatosensory stimulation for improving balance in post-stroke patients, concluding that both vibrotactile and electrotactile are an effective strategy to enhance postural stability. This is particularly relevant as the underlying sensory deficit in stroke patients, a disruption in sensory signal transmission to the brain, is comparable to that experienced by individuals with amputation. This comparability suggests that sensory feedback technologies such as electro- and vibrotactile stimulation hold potential for restoring sensation in individuals with lower extremity amputation [13, 14]. Electrotactile feedback has shown to be effective in upper extremity prosthetics for object recognition tasks [15]. This success highlights the potential of sensory feedback to substitute missing feeling and improve perception for individuals with lower extremity amputation.

Most existing systems focus on gait applications or require laboratory setups. For example, the research project SimBionics integrated sensory feedback into lower limb prostheses to support motor control, but emphasized activity-specific calibration (e.g., sitting vs. walking) and was limited to laboratory settings without CE certification [16, 17], thus limiting its practical applicability in diverse real-world scenarios. Invasive techniques, such as stimulation of residual nerves using implanted electrodes, are another option [18], but these approaches are less preferred due to surgical requirements and patient burden, preventing widespread adoption despite their potential for enhanced sensation.

1.1 Study objectives

This pilot study aims to evaluate the feasibility and preliminary effects of vibrotactile plantar pressure feedback on postural balance in individuals with a bilateral transtibial amputation, utilizing a commercially available solution. We hypothesized that applying sensory feedback would improve postural balance.

In addition, a validation study of the Suralis insole was performed to assess its feasibility for balance assessment. This involved investigating whether the Suralis insole's pressure sensor outputs could accurately and reliably reflect force plate data, thereby determining its concurrent validity and spatial accuracy for pressure measurements.

2. MATERIALS AND METHODS

This study took place at the Military Rehabilitation Centre Aardenburg and involved a single participant with a bilateral transtibial amputation. For this research, we utilized the Suralis system to investigate the feasibility and effects of vibrotactile plantar pressure feedback on postural balance. Measurements were taken using a GRAIL system to quantify balance during various functional tasks through force platform data. These measurements were performed both with and without the Suralis system activated to determine its influence on postural balance during these tasks. Because the participant discontinued the intervention during the familiarization period, the results presented are limited to baseline data and short-term effects, rather than long-term adaptation.

2.1 Prosthetic intervention setup and calibration method

The intervention system applied is the Suralis conversion kit (Saphenus Medical Technology GmbH, Vienna, Austria). The Suralis consisted of a sock with a sole that incorporates five pressure sensors. The sock was placed around the prosthetic foot within the shoe and the sleeve with four vibrating motors incorporated was placed around the thigh. From top to bottom, these motors were activated by the output of the heel sensor, the fifth metatarsal sensor, and the first metatarsal sensor, respectively. The lowest vibration motor was activated by the combined output of the toes and hallux sensors.

The insole incorporated an 8-cell high dynamic force sensing resistor (HD-FSR) insole from IEE [19]. The HD-FSR insole was specifically designed for in-shoe pressure data acquisition applications. The insole measured punctual plantar pressure of up to 7 bar beneath the heel, midfoot, metatarsal heads, and toes. The Suralis did not read the sensors of the middle foot and the third metatarsal head. Each HD-FSR cell is type HD 002 and measured a resistance change over a pressure range from 250 mbar to 7 bar. The hysteresis for the HD 002 sensor was reported 8% [19]. For each single HD-FSR sensor, we could set a threshold value for sensibility.

The participant received two Suralis sets, one for each leg. Prior to data collection, we implemented a standardised calibration protocol, based on the manufacturer's recommendations. This protocol involved individually setting the vibration duration and activation threshold for each of the four vibrotactile elements. The calibration aimed to ensure the vibrations were perceptible, yet comfortable, and activated based on a shift in the corresponding pressure sensor's output. We also calibrated the vibration motors, so the participant perceived each motor with the same intensity. Figure 2-1 presents a diagram of the Suralis system.

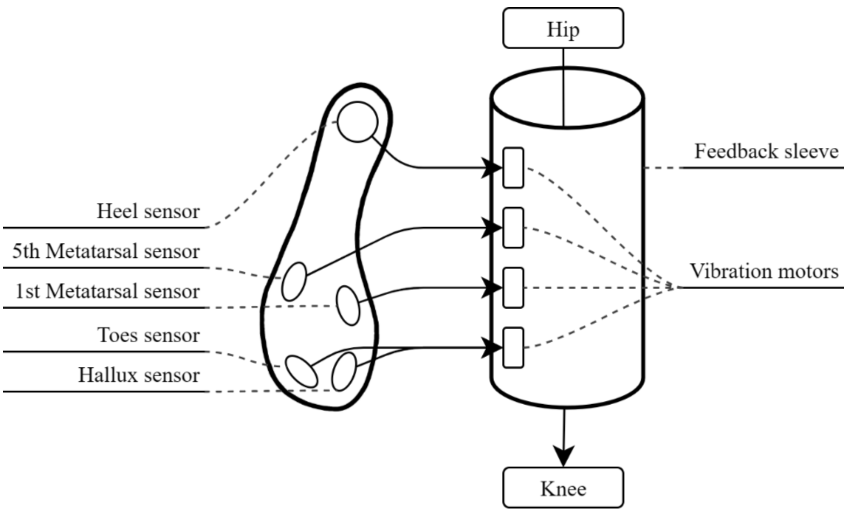

Figure 2-1: Diagram of the Suralis system. On the left, the sole with 5 pressure sensors is shown. On the right, the feedback sleeve displays 4 vertically aligned vibration motors. From top to bottom, these motors were activated by the heel sensor, the fifth metatarsal sensor, and the first metatarsal sensor, respectively. The lowest vibration motor was activated by the combined output of the toe and hallux sensors.

2.2 GRAIL-system

Data acquisition took place in a gait lab environment, utilizing the GRAIL system (Gait Real-time Analysis Interactive Lab, Motek Medical BV, Amsterdam, The Netherlands). This integrated lab environment featured a dual-belt treadmill with two embedded force platforms, a motion capture system (MoCap, Vicon Motion Systems Ltd., Oxford, United Kingdom), and a 240-degree hemisphere display. The MoCap system, operating at 100 Hz, used 10 infrared cameras and three video cameras to track participant movement via reflective markers strategically placed on anatomical landmarks according to the Vicon Plug-in Gait lower body model [20]. Simultaneously, the two integrated force platforms provided ground reaction force data for each leg at 1000 Hz. Throughout data acquisition, participants wore a safety harness for fall prevention.

2.3 Synchronization of the obtained data

Synchronization of the obtained GRAIL data (comprising force plates and marker data) with the Suralis insole system was necessary for accurate analysis. This was achieved by recording specific foot lift and drop incidences at the beginning of each data acquisition trial, which served as synchronization points across all systems.

For the GRAIL system, the force plated detected these incidences as a temporary absence of vertical ground reaction force. This occurred when the normalized vertical ground reaction force crossed a threshold of 20% bodyweight. For the MoCap system, synchronization was evident through a corresponding change in the vertical coordinate of the reflective markers placed on the foot.

For the Suralis system, which incorporated pressure sensors within the insoles, a foot lift incidence was defined as the moment when the sum of all raw Analog-to-Digital Converter (ADC) values crossed a threshold of 400 ADC from a higher to a lower value. Conversely, a foot drop incidence was defined as the moment when the sum of all raw ADC values crossed 400 ADC again, this time from a lower to a higher value.

To align the time series from both systems, the average timestamp between these two incidences (foot lift and foot drop) from the Suralis data was compared to the average timestamp of the corresponding foot lift and foot drop incidences from the GRAIL force plate signal.

2.4 Study protocol: Validation of the vibrotactile system

To validate the Suralis insole's application for postural control, three analyses were performed: a pressure force comparison, pressure distribution heatmaps, and a vibration motor activation analysis. Additionally, the centre of pressure (CoP) was estimated from the Suralis pressure sensor readings using a custom multiple linear regression model (MLR). It is important to note that this CoP estimation is an independent analytical step in our study and is not inherent to the Suralis system's real-time feedback or proprietary software.

For the pressure distribution heatmaps, vibration motor activation, and CoP estimation, participants stood on the GRAIL system's dual-belt treadmill, with one leg positioned on each integrated force plate. To ensure a standardized and stable loading condition representative of typical quiet standing, only measurements where 40-60% of the participant's total body weight was applied to each individual force plate were included for analysis. This criterion helped standardize the load and ensure consistent pressure distribution data across trials and participants.

2.4.1 Pressure force comparison

To characterize the relationship between applied weight and sensor output, a series of measurements were performed on a single pressure sensor. Known weights, ranging from 0 kg to 80 kg, were systematically applied to the sensor. This range was selected as it encompasses the operational limits of the sensors and aligns with expected pressure distribution during standing.

To simulate the dynamic weight fluctuations experienced during standing, measurements were conducted with both increasing and decreasing applied weights. For the increasing weight instances, the current applied weight was always higher than the previous weight. Conversely, for decreasing weight instances, the following applied weight was lower than the previous weight. additionally, a set of baseline measurements were taken where the previous applied weight was consistently 0 kg.

Data points suspected of involving external support, where the force was not exerted solely on the sensor, were excluded from the analysis to ensure the integrity of the measurements.

Based on the technical specifications provided in the HD-FSR sensor datasheet, the relationship is expected to be logarithmic [19].

2.4.2 Pressure distribution heatmaps

To visualize the contribution of individual pressure sensors to the overall pressure distribution across the foot sole, heatmaps were generated by overlaying sensor readings onto CoP trajectories measured by a force plate (GRAIL system). For each CoP measurement timestamp, the raw output of a specific pressure sensor was used to colour-code the corresponding CoP location. The intensity of the colour was configured to represent the magnitude of the sensor's reading, allowing for a qualitative assessment of sensor activation patterns.

The pressure distribution heatmap aimed to assess the alignment between the pressure distribution measured by the Suralis insole and the CoP observed by the GRAIL system. Only measurements where 40-60% of the participant's body weight was applied to a single force plate were included to standardize the load condition and ensure a consistent representation of pressure distribution.

2.4.3 Vibration motor activation analysis

To evaluate the functionality and consistency of the haptic feedback system, the activation patterns of the vibration motors were analysed in relation to the CoP locations. For each sensor, a threshold defined in Table C.1 determined whether its corresponding vibration motor would activate. The CoP locations were then color-coded to visually indicate whether the vibration motor associated with a specific sensor (e.g., heel, hallux, toes) was activated or not activated. This analysis aimed to identify if the haptic feedback system provided consistent cues based on pressure changes. To ensure a consistent representation of the activation, only measurements where 40-60% bodyweight was applied to each leg were included.

2.4.4 CoP estimation from pressure sensor readings

To estimate the CoP from the Suralis pressure sensor readings, a MLR model was employed. This model aimed to determine optimal weights for each sensor, quantifying their influence on the overall CoP in both the ML (x) and AP (y) directions. The CoP locations with 40-60% bodyweight obtained from the GRAIL force plate system were utilized as the "true" or observed CoP for model training and validation.

The estimated CoP coordinates $\mathrm{CoP_x}$ and $\mathrm{CoP_y}$ were calculated as a weighted average of individual sensor pressure readings ($\mathrm{P_i}$). The calculations are given by the relations

$$\mathrm{CoP_x} = \frac{\sum_{i=1}^{n}(\mathrm{P_i} * \mathrm{W_{xi}})}{\sum_{i=1}^{n}(\mathrm{P_i})}, \qquad \mathrm{CoP_y} = \frac{\sum_{i=1}^{n}(\mathrm{P_i} * \mathrm{W_{yi}})}{\sum_{i=1}^{n}(\mathrm{P_i})} \qquad \text{Equation 1}$$

where $\mathrm{W_{xi}}$ and $\mathrm{W_{yi}}$ represent the weights for each sensor i in the x and y directions, respectively, as determined by a MLR model. The variable n denotes the total number of pressure sensors.

The accuracy of the estimated CoP was quantified using the Root Mean Squared Error (RMSE), which represents the average difference between the CoP predicted by the Suralis system and the CoP observed by the GRAIL. In addition, the RMSE was expressed as a percentage of the dynamic range of the measured CoP, calculated as the difference between the maximum and minimum observed CoP values (i.e., %RMSE). Furthermore, a visual comparison of the estimated and observed CoP trajectories was also generated as a video, accessible via a provided YouTube link.

2.5 Study protocol

Before receiving the Suralis conversion kit, the participant completed the Activities-specific Balance Confidence (ABC) Scale, a validated questionnaire that assesses how confident they feel performing everyday activities without losing balance [21]. This was followed by a demographic questionnaire that recorded background information, such as weight, length, and relevant medical history.

Thereafter, the participant received the Suralis, and an experienced certified prosthetist assessed the fitting, ensuring that it fitted comfortably and securely. Once the fit was confirmed, the Suralis system was calibrated while the participant stood. The vibrotactile feedback was fine-tuned to align with the participant's unique pressure distribution, ensuring the system functioned as intended. With the Suralis fitted and calibrated, the Berg Balance Scale (BBS) [22] was executed with the participant while the intervention was turned off. The ABC scale [21], BBS [22] and a questionnaire for demographic data served as baseline contextual measures.

2.6 Intervention procedure

The data acquisition was executed by ABAB introduction/withdrawal design [23]. First, the baseline data acquisition of the experiment was executed, i.e. Phase A. Hereafter, the vibrotactile feedback intervention was introduced by turning on the Suralis system, phase B. Each trial included two times phase A and two times phase B, as shown in Figure 2-2.

A total of four trials with the same design was executed, the only difference was the task requested:

1. Standing with eyes open (EO),
2. Standing with eyes closed (EC),
3. Standing while performing a cognitive dual task (CT), and
4. Standing during a reach-and-target task (RTT).

Each phase lasted 1.5 minutes. Each of the four trials always consisted of four phases and thus lasted six minutes. After each trial, the subject was given three minutes of rest before the next trial and was allowed to sit during this downtime. In combination with transfers and downtime the data acquisition took approximately 45 minutes.

Following the baseline data acquisition and four weeks of familiarization at home, a follow-up data acquisition using the same protocol as baseline was scheduled.

2.6.1 Cognitive dual task

To investigate the interplay between cognitive processing and postural control, participants were instructed to prioritize maintaining a stable upright stance while simultaneously performing a Stroop test during the third trial. By emphasizing the postural task, researchers could gain insights into how cognitive load affects the automaticity of balance control mechanisms [24].

2.6.2 Reach and target task

The reach and target task (RTT) chosen was the "kite flyer" application on the GRAIL system. Within this task, the participant holds one stick in both hands. Using trunk movements, the stick controls a kite. The participant collected static tokens (targets) in the air while dodging two other moving kites. The RTT was incorporated in the fourth trial to evaluate dynamic postural control. Reaching movements inherently challenged stability, requiring the individual to adjust their centre of mass (CoM) [1]. This type of task allowed for the data acquisition of balance responses during goal-directed actions, which are relevant to everyday activities.

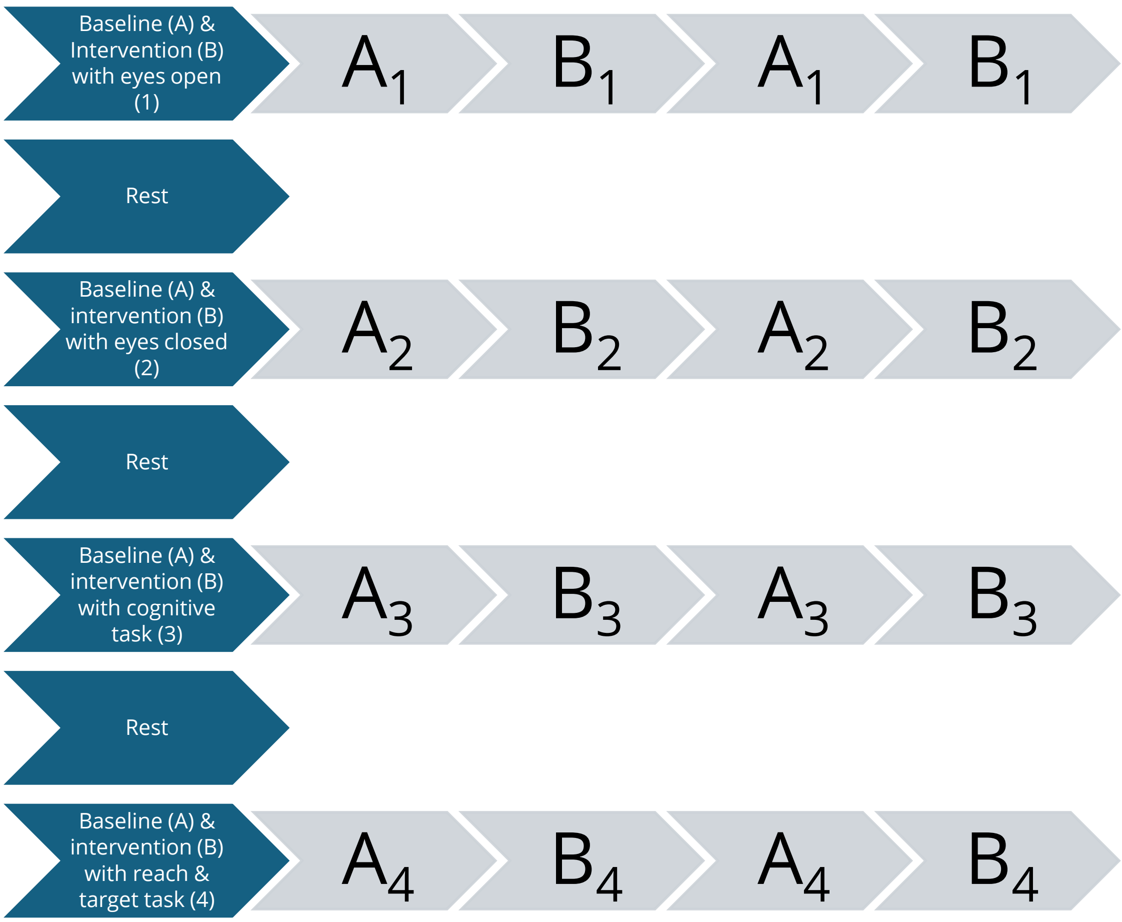

Figure 2-2: Repeated ABAB introduction/withdrawal design with 4 standing tasks. The first and third grey column represent phase A, in which the intervention is turned off. The second and fourth grey column represent phase B, in which the intervention is turned on. Each grey row represents a new trial, indicating the task number that was applied in that trial.

2.7 Outcome measures

The primary outcome measures were:

1. The centre of pressure speed (CoPs), calculated as the total distance covered by the CoP trajectory within the time window corresponding to each experimental phase, divided by that window's duration. The CoPs was extracted from the measured CoP location trajectory obtained from the GRAIL force plates. CoPs was expressed in millimetres per second (mm/s).

2. The Margin of Stability (MoS), defined as the shortest distance between the extrapolated centre of mass (xCoM) and the edge of the base of support (BoS) at each timestamp. The average MoS was determined for both the AP and medio-lateral (ML) directions within the time window corresponding to each experimental phase. The MoS was expressed in millimetres (mm).

   The xCoM was computed as the projection of the velocity adjusted CoM onto the stance plane [25]. All marker positions, including those for CoM and BoS, were recorded using a MoCap system with the Vicon Plug-in Gait lower body model. The CoM itself was defined by the average position of four pelvic markers. We determined the CoM velocity in both the ML and AP directions by computing the first derivative of the CoM position data with respect to time. Prior to velocity calculation, missing data for the pelvic markers were reconstructed using local coordinate system interpolation. Subsequently, any remaining gaps in all marker data were filled using linear interpolation.

To determine the edge of the BoS, all six markers placed on the feet were used. The BoS was defined as the edge of the rectangle formed by connecting these marker positions.

For the BoS, six markers were placed on the feet to define its edge. The stance plane's boundary was computed per time instance, and the BoS was defined as the rectangle formed by the most anterior, posterior, and lateral coordinates of these six marker positions.

During de data acquisition, participants kept their shoes on, as their prostheses were calibrated to these shoes. Tape applied to the GRAIL system confirmed a consistent foot placement, which was maintained throughout the data acquisition session.

3. RESULTS

This study included data from a 54-year-old male with bilateral transtibial amputation caused by vascular disease, who used bone-anchored prostheses on both sides and was classified as a very active, K4 adult. Baseline contextual measures are available in Appendix B, and the resulting vibration thresholds obtained by the calibration protocol are presented in Appendix C. Furthermore, we successfully synchronized the Suralis signals for each phase with the GRAIL, as shown in Appendix D. The results of the Stroop test from the CT trial and the kite flyer application from the RRT trial are placed in Appendix F.

3.1 Pressure force comparison

The relationship between applied weight and the raw pressure sensor output for a single sensor is depicted in Figure 3-1. The data revealed a clear logarithmic relationship between the applied weight and the sensor's output. As the applied weight increased, the curve's slope decreased, indicating a flattening of the raw output value difference at higher weights.

The analysis of the lower weight range (0-20 kg) was of particular interest due to the observed maximum raw ADC values of 180 in pressure distribution heatmaps below, suggesting that individual sensors would typically experience lower pressures during standing. Figure 3-2 provides a zoomed-in view of this range, highlighting the steeper part of the curve.

We observed variability in the output, especially for sensor outputs above 200 ADC. For instance, a sensor output of 212 ADC corresponded to an applied weight ranging from 10 kg to 17.5 kg, while an output of 222 ADC represented a weight in the range of 12.5 kg to 20 kg.

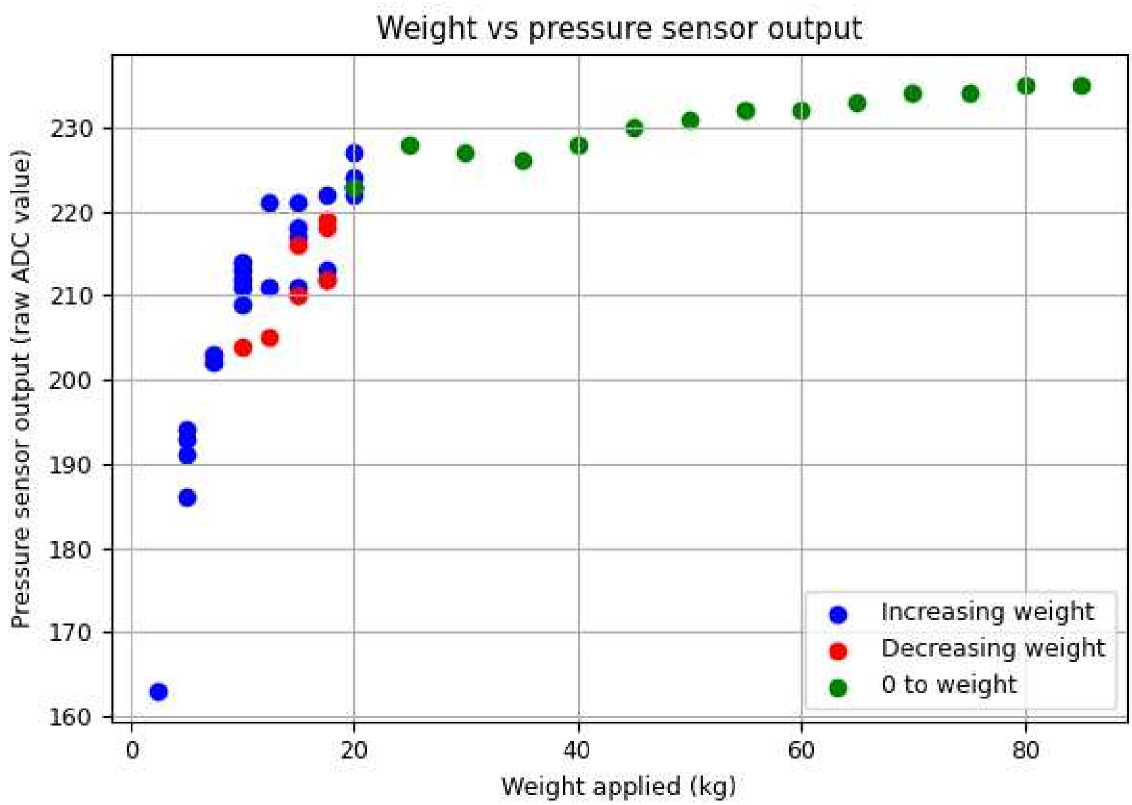

Figure 3-1: Weight applied to and pressure sensor output of a single pressure sensor.

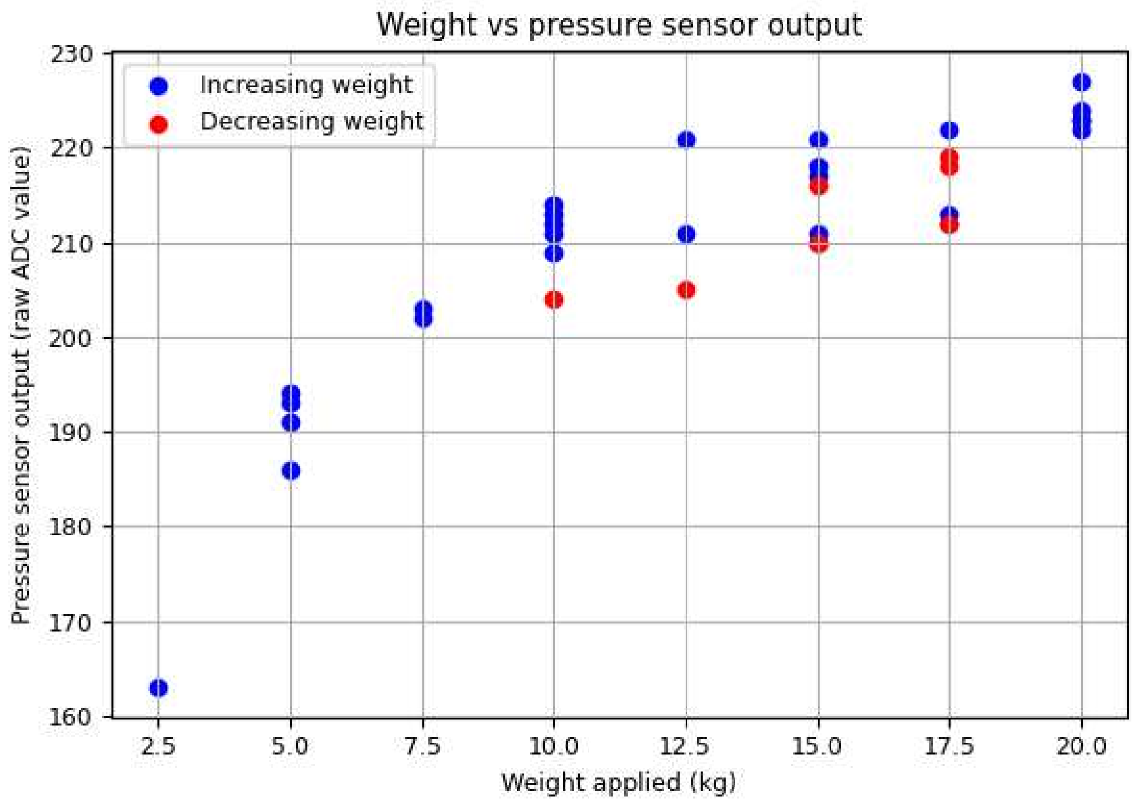

Figure 3-2: Relevant part of the force vs pressure of a single sensor.

3.2 Pressure distribution heatmaps

The pressure distribution under the foot during baseline data acquisition was illustrated through heatmaps, where the colour of each CoP location dot reflects the raw output of individual pressure sensors. Higher sensor output is represented by green, while lower output is represented by red.

Figure 3-3 displays the CoP locations, measured by the GRAIL system during the first data acquisition across all four trials, coloured by the raw pressure sensor output of the toes sensor. Similarly, Figure 3-4 and Figure 3-5 present the CoP locations coloured by the raw outputs of the hallux and heel sensors, respectively. Figures for the first and fifth metatarsal sensors are provided in Appendix E.

Visual inspection of these heatmaps (Figure 3-3, Figure 3-4, Figure 3-5, Figure E-1, and Figure E-2) reveals a clear relationship between the CoP location and the corresponding individual pressure sensor readings. The output of a sensor generally increased as the CoP approached its physical location and decreased as the distance grew. This observation confirmed that each sensor provided a distinct output related to its proximity to the applied pressure.

However, the operational range and activation patterns varied among the pressure sensors. Specifically, the sensors located under the toes and hallux frequently registered a value of zero, indicating periods of no or minimal pressure. In contrast, the sensors under the heel, first, and fifth metatarsals consistently showed some output value, even when the CoP was not directly over them. Across all sensors, the sensor values rarely exceeded 170 ADC.

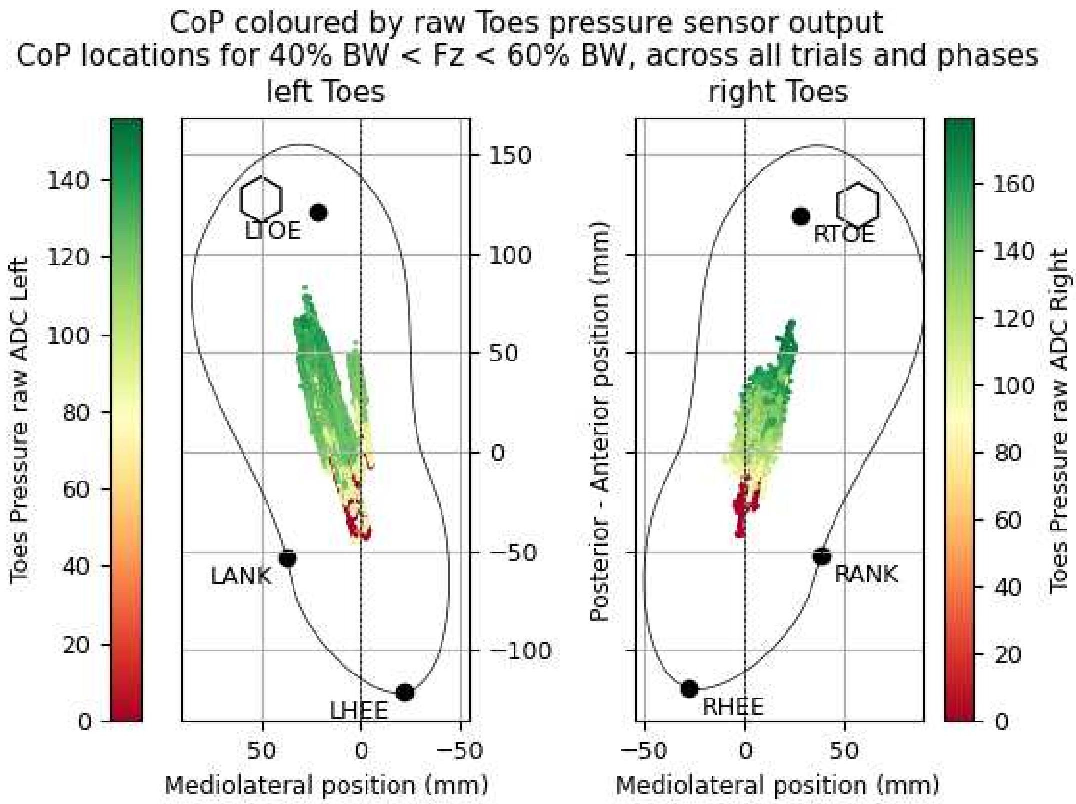

Figure 3-3: CoP coloured by the raw toes pressure sensor output during the first data acquisition, across all four trials and phases.

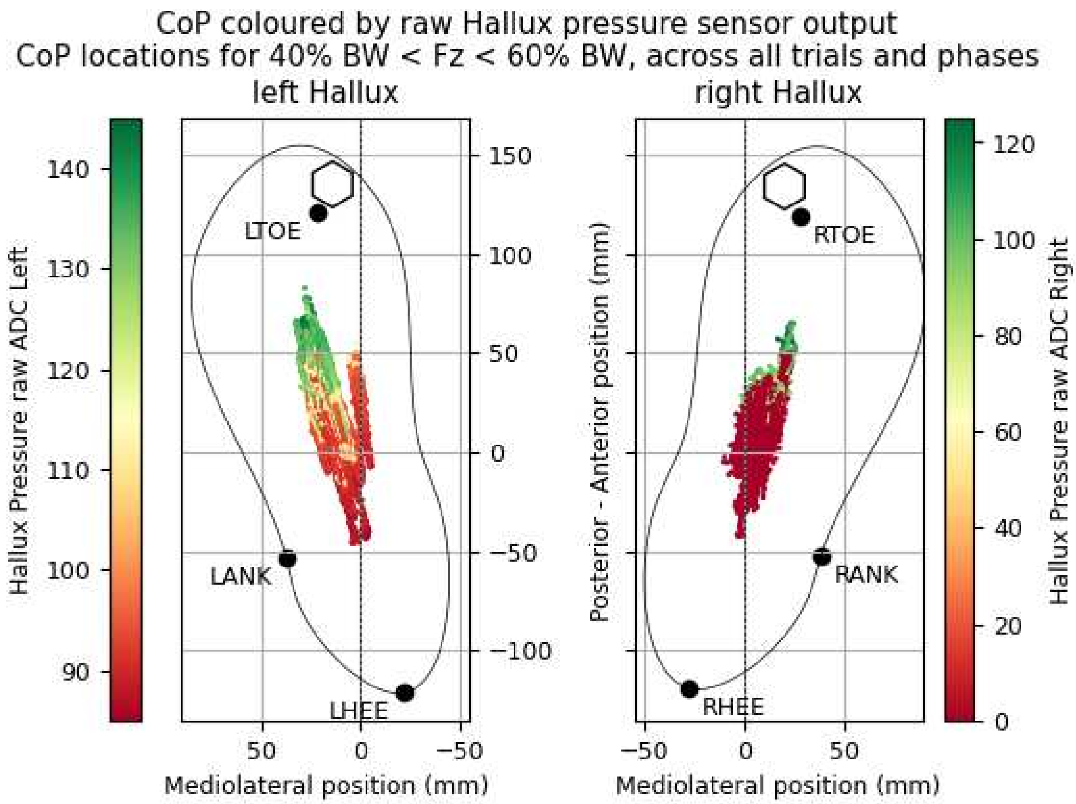

Figure 3-4: CoP coloured by the raw hallux pressure sensor output during the first data acquisition, across all four trials and phases.

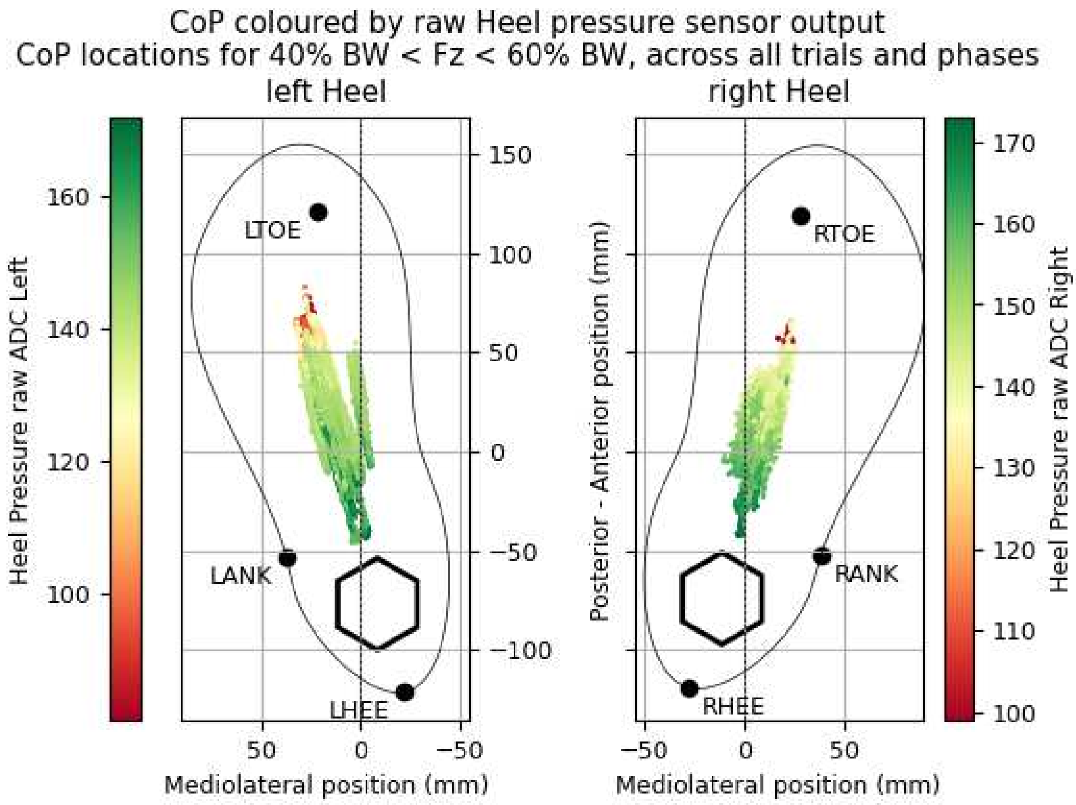

Figure 3-5: CoP coloured by the raw heel pressure sensor output during the first data acquisition, across all four trials and phases.

3.3 Vibration motor activation patterns

Analysis of the vibration motor activation, based on predefined thresholds (Appendix C), showed inconsistencies in their triggering locations. Figure 3-6 and Figure 3-7 illustrate the CoP locations where the vibration motors for the heel, and the hallux and toes sensors, respectively, were activated (indicated by orange dots). Conversely, Figure 3-8 and Figure 3-9 focus on the CoP locations where these motors were not activated (indicated by black dots).

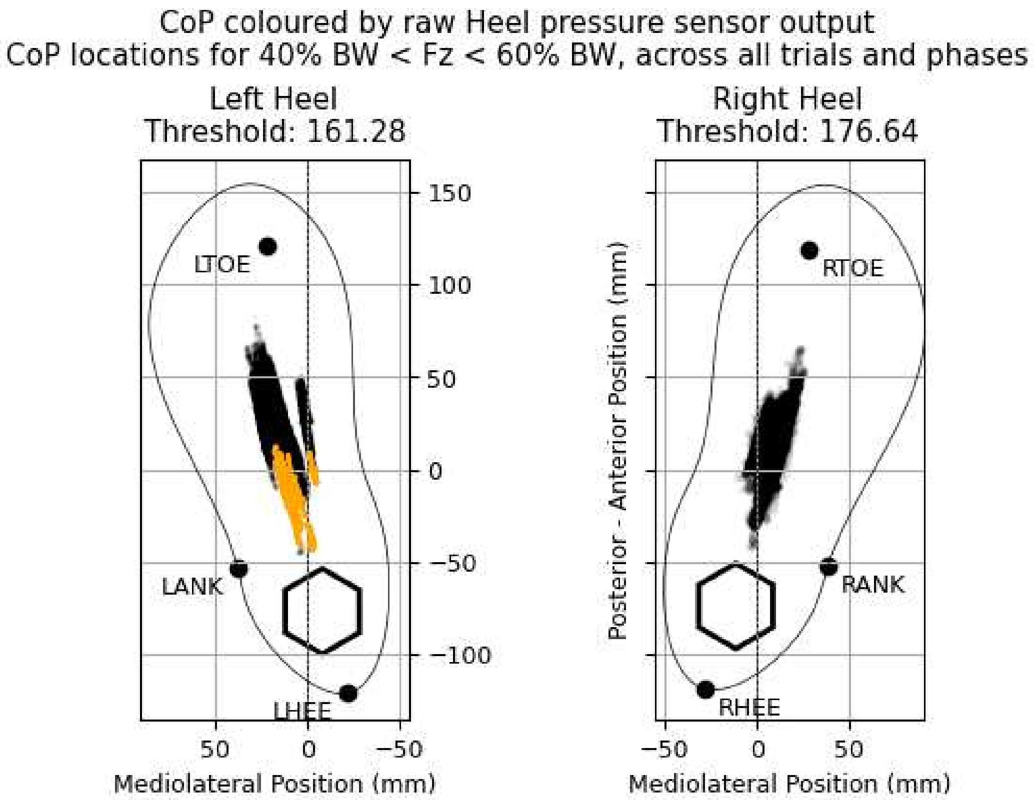

Figure 3-6: Heel vibration motor activation at the corresponding CoP locations. Orange indicates activation of the vibration motor.

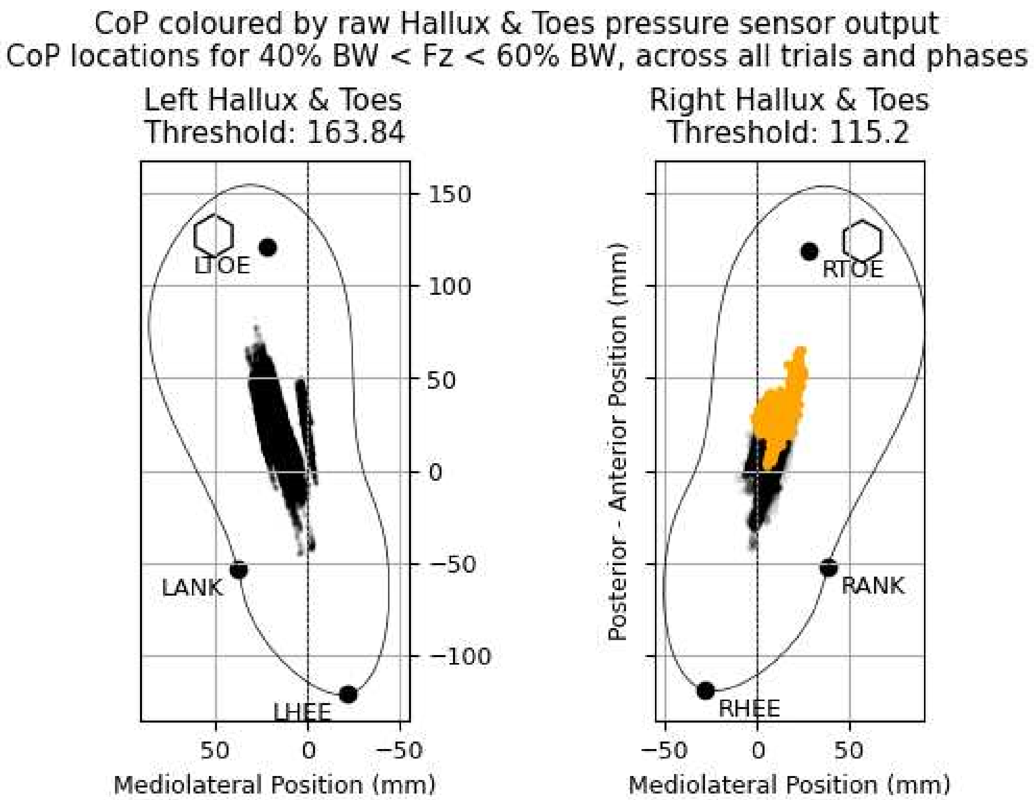

Figure 3-7: Hallux and Toes vibration motor activation at the corresponding CoP locations. Orange indicates activation of the vibration motor.

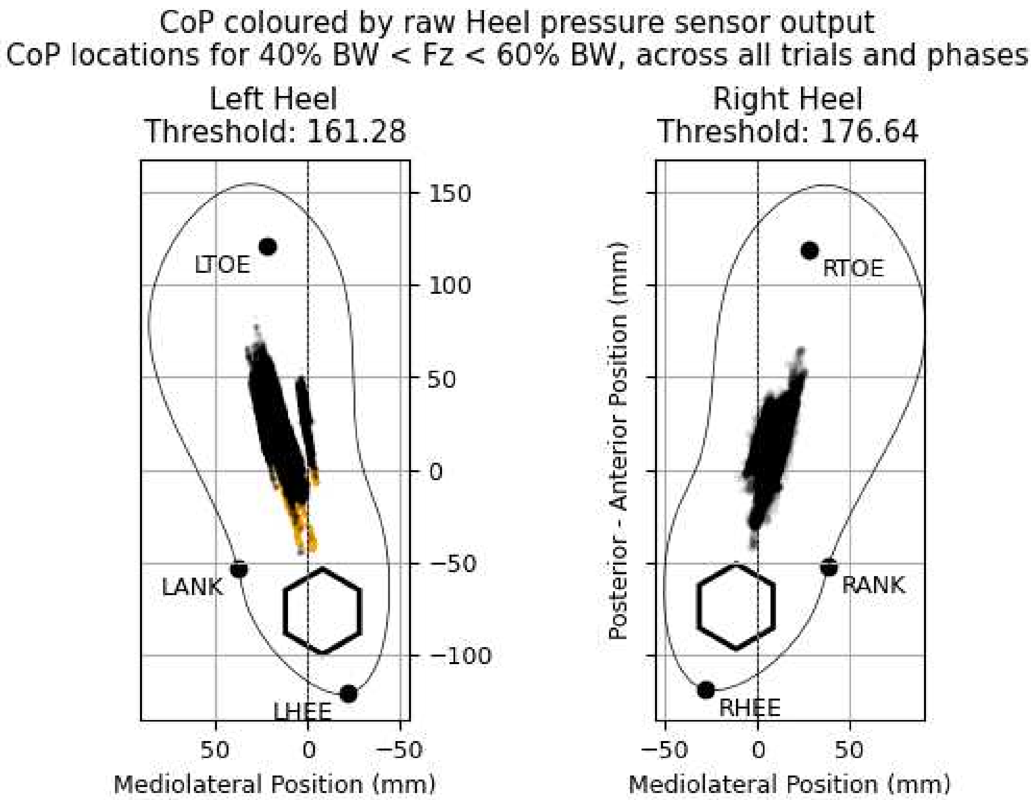

Figure 3-8: Heel vibration motor activation at the corresponding CoP locations. Black indicates where the heel vibration motor was not activated.

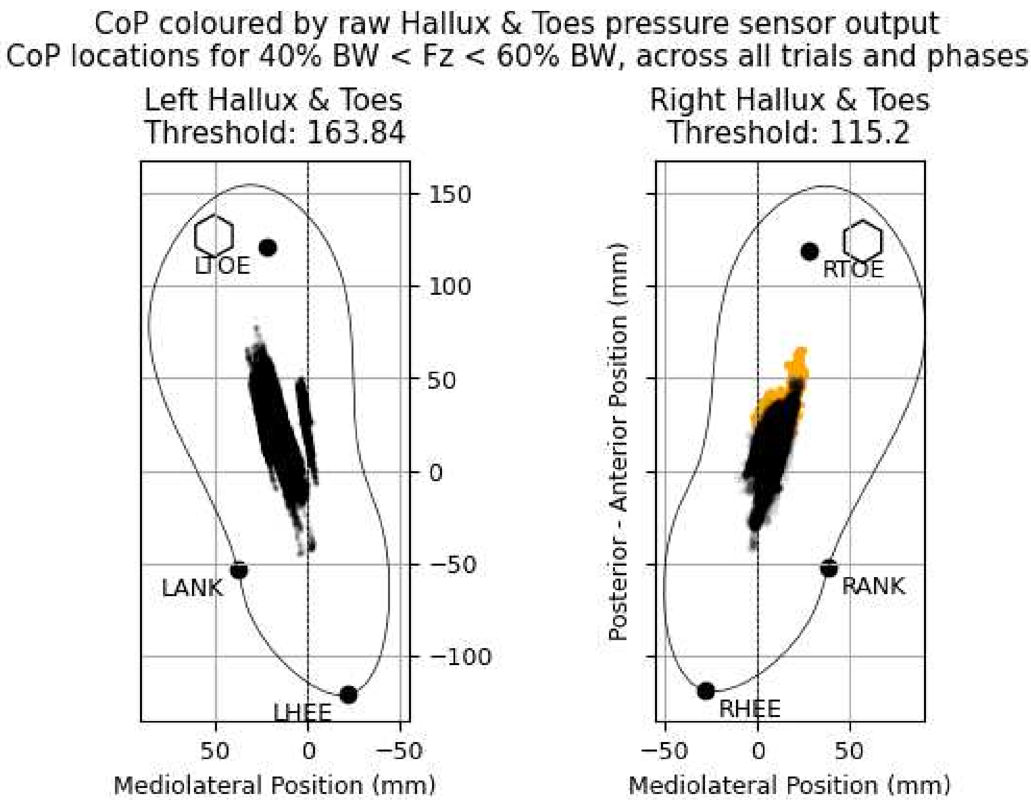

Figure 3-9: Hallux and toes vibration motor activation at the corresponding CoP locations. Black indicates where the Hallux and toes vibration motor was not activated.

A direct comparison across these four figures (Figure 3-6, Figure 3-7, Figure 3-8, and Figure 3-9) highlighted that the location at which a vibration motor exceeded its threshold and therefore activates is not consistent. Moreover, the left hallux and toes, and the right heel vibration motors, appeared to be never activated during the standing tasks.

3.4 CoP estimation

The optimal weights for each Suralis pressure sensor, determined by the MLR model for estimating CoP in both x (ML) and y (AP) directions, are presented in Table 3.1. The left foot was positioned in the second quadrant, and the right foot in the first quadrant during data acquisition. The weights for the heel were negative while the weights for the toes were positive, but small.

Table 3.1: Optimal weights found by the MLR model. Note that the left foot is in the second quadrant and the right foot is in the first quadrant. W_{xi} and W_{yi} are the weights, expressed as scalar values, as determined by the MLR model for pressure sensor i respectively in x or y direction.

Sensor (i)	*Left* W_{xi}	*Left* W_{yi}	*Right* W_{xi}	*Right* W_{yi}
Heel	-46.74	-415.47	-151.26	-563.78
Fifth Metatarsal	-191.34	-581.66	337.76	647.53
First Metatarsal	136.74	801.06	-164.40	-79.78
Toes	67.28	77.95	14.54	27.62
Hallux	144.91	216.89	6.77	32.30

The accuracy of the CoP estimation was quantified by the RMSE, presented in Table 3.2. The RMSE values indicated the average difference between the Suralis-predicted CoP and the GRAIL-observed CoP. Overall, the CoP estimation achieved an RMSE of less than 10 mm in all directions, with higher RMSE values observed in the AP directions. RMSE values were also expressed as a percentage of the observed CoP range (%RMSE). These relative errors ranged from 5.27% to 13.43%, with higher percentages observed in the ML direction.

Table 3.2: RMSE of the CoP predicted by the Suralis and the observed CoP by the GRAIL.

Side and direction	*RMSE*	*%RMSE*
Left CoPx (ML)	5.17 mm	13.43%
Left CoPy (AP)	9.01 mm	7.00%
Right CoPx (ML)	3.35 mm	9.24%
Right CoPy (AP)	5.67 mm	5.27%

A visual comparison of the estimated CoP (from Suralis) and the observed CoP (from GRAIL) is provided in Figure 3-10. This figure displayed the trajectories, showing the alignment between the two methods. For the AP direction (CoP y), the data points for both the left and right feet showed alignment close to the y=x line. In contrast, the data points for the ML direction (CoP x) for both feet appeared to follow a flatter or more horizontal trend.

The estimated CoP in comparison to the observed CoP was visualized in a video for trial EC phase B1, available at:

https://youtu.be/j62oTRKDOZ0 Video 1: Link to CoP comparison, YouTube

Visual inspection of the synchronized video, which included the Suralis-approximated CoP alongside the GRAIL-calculated CoP, demonstrated a close visual agreement between the two measurements. Occasionally, brief deviations of the Suralis approximation from the GRAIL CoP were observed.

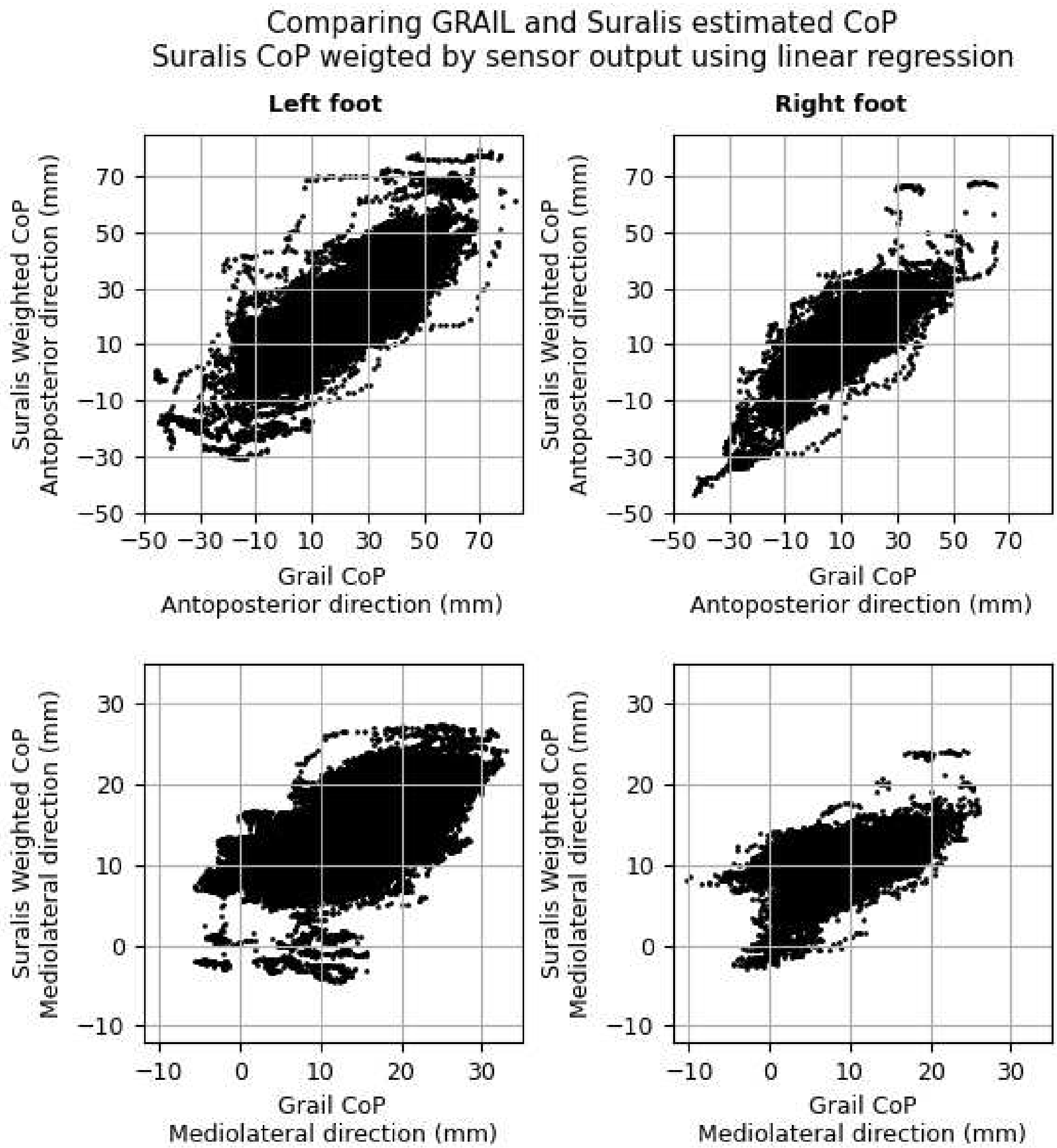

Figure 3-10: Comparison of the CoP as calculated by the GRAIL and the CoP as estimated by the Suralis pressure sensor readings. The weights are determined through MLR.

3.5 Effects in CoPs

CoPs was calculated as the total distance covered by the CoP during a phase, divided by the phase duration. The unit used is millimetres per second (mm/s). In Figure 3-11, boxplots were constructed to visualize the distribution of the outcomes. The four trials with their phases can be found on the x-axis. The top row showed the CoPs for the left foot, while the bottom row showed the CoPs for the right foot.

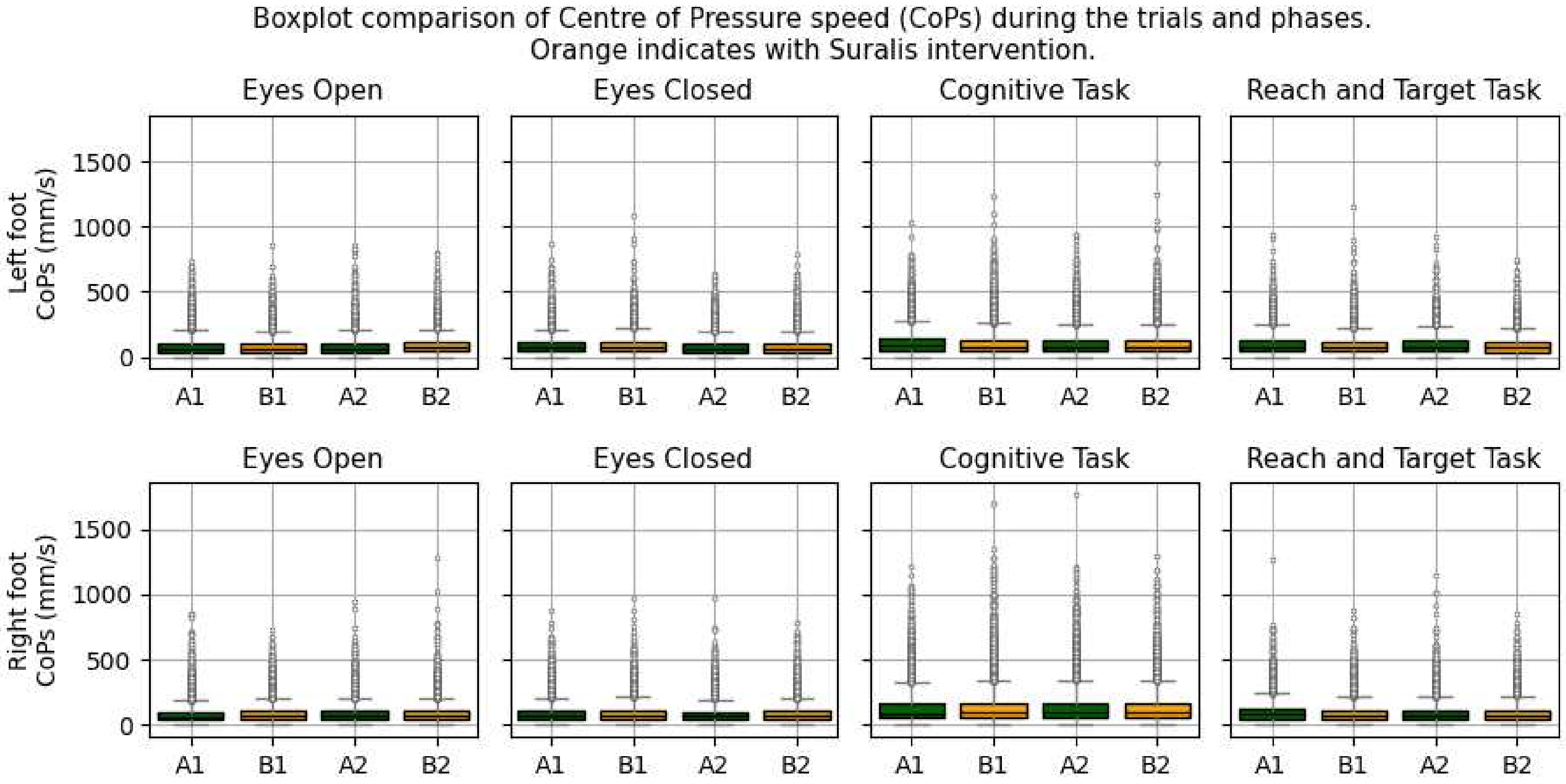

Figure 3-11: Boxplots of the CoPs per phase.

Figure 3-12 provides a zoomed-in view of the CoPs boxplots. Within each boxplot, the 'x' mark denoted the mean CoPs for that phase, while the horizontal line indicated the median. CoPs were observed to increase and have a higher interquartile range in the CT trial compared to the EO trial. The patterns of CoPs, including the mean, median, and spread, were consistent between the left and right foot. Individual data points plotted as circles beyond the whiskers of the boxplots were observed in Figure 3-11, indicating outliers, with an increased density and magnitude of these outliers particularly in the CT trials.

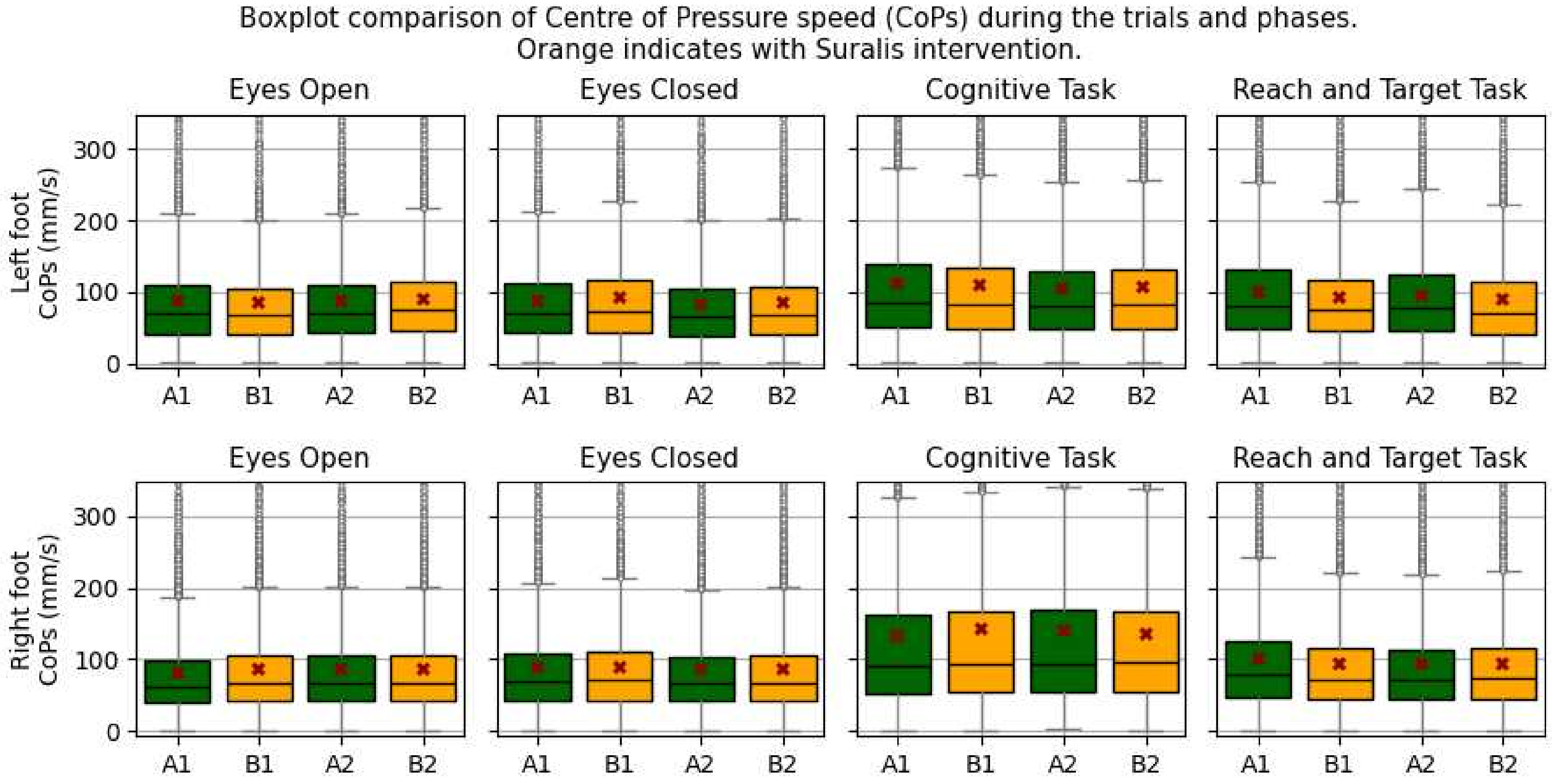

Figure 3-12: Zoomed in on CoPs boxplots. Within each phase, ‘x’ marks the mean CoPs.

3.6 Effects in MoS

Figure 3-13 presents boxplot comparisons of the MoS during the first data acquisition, across all four trials and phases. MoS, measured in millimetres (mm), quantified the distance between the xCoM and the edge of the BoS. A larger MoS indicated greater stability. The boxplots visualized the distribution of MoS outcomes, with orange boxes specifically indicating phases with Suralis intervention. The top row showed MoS in the AP direction, while the bottom row displayed MoS for the Medio-Lateral (ML) direction.

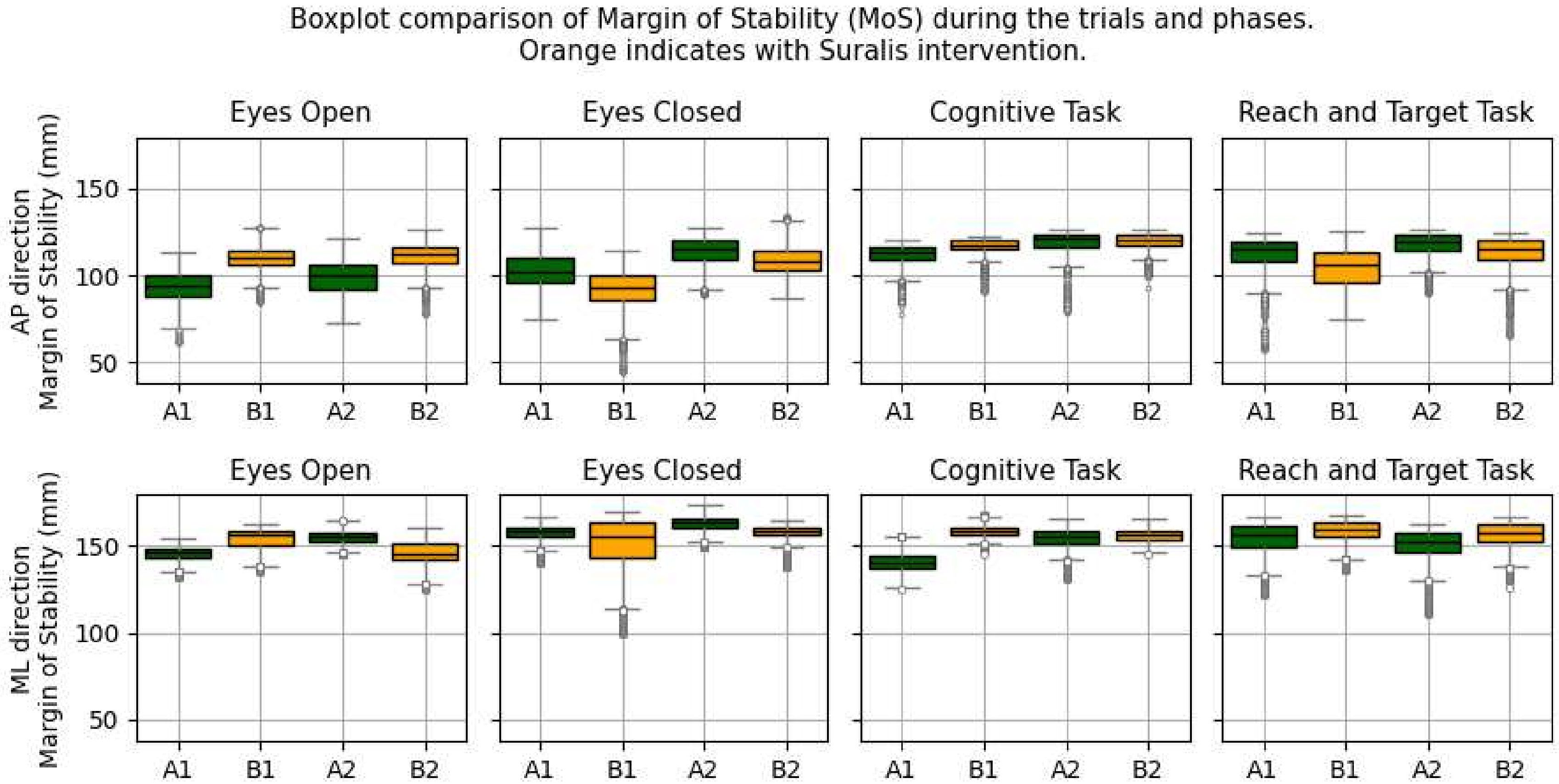

Figure 3-13: Boxplots of the MoS per phase.

Figure 3-13 illustrates that median MoS values were consistently lower in the AP direction compared to the ML direction across all trials. Furthermore, a larger interquartile range was observed in the AP direction compared to the ML direction across all trials.

Regarding the Suralis intervention, indicated by the orange boxes, a slight increase in AP MoS was observed in the EO trial compared to its corresponding non-intervention phase. This observation did not persist in more challenging tasks (EC, CT, and RTT). Notably, in both the EC and RTT trials, phases with the Suralis intervention demonstrated a reduction in AP MoS compared to their respective baseline phases.

A consistent pattern observed during the first data acquisition across all trials was an increase in AP MoS from phase A1 to A2, and similarly from phase B1 to B2.

4. DISCUSSION

This study aimed to investigate the extent to which the Suralis system serves as a valid tool for measuring postural balance and delivering vibrotactile plantar pressure feedback in individuals with bilateral lower extremity amputation. The results presented are solely from baseline data acquisition. This allowed for a detailed assessment of the Suralis insole's fundamental capabilities and limitations for measuring plantar pressure distribution during standing tasks.

4.1 Suralis as a tool for measuring postural balance

The Suralis system's potential for measuring postural balance in individuals with bilateral lower extremity amputation relies on its ability to quantify plantar pressure distribution during standing. Our findings indicated that individual pressure sensors exhibited a logarithmic relationship between applied weight and raw sensor output (Figure 3-1). This non-linear response suggests that sensors are more sensitive at lower pressure ranges, where a given change in weight results in a larger change in sensor output. This enhanced sensitivity at lower pressures is relevant for monitoring subtle shifts in the CoP, which is a key indicator of postural stability during standing [26, 27].

The pressure distribution heatmaps (Figure 3-3, Figure 3-4, Figure 3-5, Figure E-1, and Figure E-2) demonstrated the Suralis system's ability to localize pressure. We observed that sensor output increased as the CoP approached a sensor's location and decreased as the distance grew, confirming the system's capacity to map pressure distribution across the foot during standing. These observations align with common balance strategies, particularly how weight is distributed across the foot. For instance, sensors under the toes and hallux frequently registered minimal or zero values, indicating these regions may not consistently bear significant sustained pressure. Conversely, sensors under the heel, first, and fifth metatarsals consistently showed some output. This consistent presence of readings in these regions, even when the CoP was not directly over them, supports the idea of broad weight distribution across the sole to maintain stability, a principle consistent with how the body manages balance during quiet standing [26].

However, the variability in sensor output, particularly for ADC values above 200 (Figure 3-2), presents a challenge to the Suralis its quantitative precision for balance measurement. As seen, an output of 212 ADC could correspond to a weight range of 10-17.5 kg, and 222 ADC to 12.5-20 kg. This inherent variability makes precise weight quantification difficult. This challenge with achieving high precision across different pressure ranges is a known aspect of insole-based pressure measurement systems [28]. Despite this potential limitation, the overall low ADC values (rarely exceeding 170 ADC) observed across all sensors during standing tasks indicate that individual sensors generally experienced minimal applied force, operating primarily within the more sensitive, lower range of their force-response curve where this specific variability is less pronounced. Even though lower forces show less variability in sensor output, quantitative accuracy and reliability for sensor output while standing remains a concern, as achieving high precision and adequate resolution, particularly at the lower end of the pressure range, is a known challenge for insole-based systems [28].

4.2 Suralis as a tool for delivering vibrotactile plantar pressure feedback

The effectiveness of the Suralis system in providing vibrotactile plantar pressure feedback depends on the consistent activation of its vibration motors. Our analysis revealed inconsistencies in motor activation patterns during standing tasks (Figure 3-6, Figure 3-7, Figure 3-8, and Figure 3-9). Several factors could account for this inconsistency, including the inherent variability in the sensor output. Additionally, uneven weight distribution under the feet may contribute. For example, in a 100 kg participant, a 60/40% weight split between the left and right foot translates to a 20 kg difference in the force applied over the entire foot surface. These loading imbalances could plausibly explain the observed inconsistencies in the vibrotactile activation patterns.

The vibration motors for the left hallux and toes, and the right heel, appeared to be never activated, despite the presence of CoP in their respective environments. These observations suggest that the predefined activation thresholds (Appendix C) may not be optimally tuned for the pressure ranges experienced by the sensors during quiet standing or balance shifts. The consistent low ADC values observed from the pressure sensors indicate that the forces exerted on individual sensors frequently fall below these set thresholds, resulting in a lack of feedback. The complexity of setting optimal thresholds for vibrotactile feedback is further highlighted by research from Wentink et al. [9, 10], which explores the perceptual aspects of vibrotactile stimulation. Their work suggests that generic thresholds may not account for individual variations in pressure distribution or sensitivity in people with amputation, indicating a need for personalized or adaptive thresholds.

For individuals with bilateral lower extremity amputation, reliable vibrotactile feedback is important for enhancing somatosensory information and potentially improving postural control. This is crucial given that Nanivadekar et al. [4] and Eapen et al. [14] emphasize the significant role of sensory feedback in improving function and rehabilitation outcomes for people with lower extremity amputation. If the feedback is inconsistent or absent in relevant pressure zones, its utility as a balance aid is severely compromised, directly undermining the goal of restoring somatosensory information. This indicates that while the concept of vibrotactile feedback based on plantar pressure is relevant for this population, the current implementation within the Suralis system requires refinement for effective postural balance training.

4.3 Suralis as a tool for estimating CoP

Our study successfully estimated the CoP from Suralis pressure sensor readings using an MLR model, achieving RMSE values below 10 mm (Table 3.2). This level of accuracy, further supported by the visual agreement shown in Video 1, indicates that the Suralis system, when combined with an analytical model like the MLR model employed in this study, can provide a robust estimation of CoP location during standing tasks. Given that CoP is a fundamental metric for assessing postural balance, this finding supports the Suralis its potential as a tool for measuring balance in individuals with bilateral lower extremity amputation [26]. A critical methodological consideration in applying MLR was the exclusion of an intercept from the model, a constraint imposed to reflect the physical reality that the CoP is undefined when the total applied pressure is zero. This MLR-based estimation approach is important because, as discussed in the previous section, the individual Suralis pressure sensors can exhibit inconsistencies in activation and are not suitable for providing a direct, singular measure of CoP. Instead, our MLR approach leverages the collective output of these sensors to accurately and comprehensively represent a participant's balance.

The visual comparison presented in Figure 3-10 provides insight into the performance of the CoP estimation. Ideally, perfect agreement between the Suralis-estimated CoP and the GRAIL-observed CoP would result in data points falling precisely on the y=x line. The plots demonstrate that for the AP direction (CoPy) for both feet, the points generally align with the y=x line, albeit with some scatter, consistent with their respective RMSE values. In contrast, for the ML direction (CoPx) for both feet, while the RMSE values are lower (Table 3.2) indicating good accuracy, the data points visually appear to lie on a flatter or more horizontal line than the ideal y=x line. This visual characteristic is consistent with the generally smaller ML range of CoP movement compared to the AP range inherent to the foot's anatomical dimensions (i.e., foot width being smaller than foot length). This suggests that the Suralis, when integrated into this estimation framework, captures a more compressed dynamic range for the observed CoP excursions in the ML direction compared to the AP direction.

The analysis revealed that the pressure sensors within the insole are not independent. This is an expected physiological finding, as weight shifts across the foot during standing balance, pressure changes correlatively across multiple sensors. Even with this interdependence, MLR is well-suited for this analysis as it is specifically designed to account for shared variance among correlated predictors.

MLR is designed to account for the shared variance among correlated predictors, thereby accurately determining each sensor's unique contribution to the overall CoP estimate while simultaneously considering the influence of other sensors. The observed negative weight for the left fifth metatarsal sensor in the AP (y) direction (Table 3.1) exemplifies this. Rather than signifying a direct backward shift from that specific sensor, this negative weight likely represents a compensatory effect within the model, mathematically balancing strong positive contributions from other regions, specially of the first metatarsal, to optimize the overall CoP prediction.

The spatial accuracy of the CoP estimated using the Suralis system in conjunction with our MLR model was consistently high across all balance tasks. The RMSE was well below 10 mm for both feet and both movement directions. When normalized to the range of the force plate CoP signal, this corresponds to %RMSE values of max 13.34% in the ML and 7.00% in the AP direction. These results highlight that, although the absolute estimation error is small, the relative error becomes more pronounced in the ML direction, where CoP excursions during static balance are limited by anatomical constraints, specifically, the width of the foot.

To contextualize these findings, we compared them to recent literature. Jamali et al. [29] evaluated the accuracy of a kinematic-based CoP estimation method during over-ground gait using MoCap data and found higher absolute RMSEs of 17.5 mm in ML direction and 35.5 mm in AP direction. However, their associated %RMSEs were 4.46% and 3.25%, respectively. The lower relative errors in Jamali's study can be attributed to the substantially larger CoP excursions inherent to walking compared to static balance tasks, which dilute the impact of a given absolute error. Conversely, our balance tasks featured smaller overall CoP ranges, which inherently yield higher %RMSE values for a similar or smaller absolute deviation. It is also important to note that Jamali et al. included 10 healthy participants in their study, whereas our study was a case study focusing on individuals with lower extremity amputation. While our study's scope differs, the achieved absolute RMSEs below 10 mm are indicative of a strong foundation for clinical applications focused on postural control.

4.4 Suralis its effects on CoPs

Figure 3-11 and Figure 3-12 illustrate the characteristics of CoPs, which quantified the magnitude of postural sway. Tasks involving cognitive load demonstrated a substantial increase in mean CoPs, indicating impaired postural stability under dual-task conditions. This finding aligns with existing literature, as Dhillon et al. [2] directly assesses dual-task interference in postural control in people with lower limb amputation, reporting similar negative impacts on stability. Our observations reinforce the challenges that individuals with amputation face in dual-task environments, a phenomenon well-documented by structured reviews such as that by Morgan et al. [24], which broadly covers dual-task standing and walking in people with lower limb amputation.

The individual data points plotted as outliers in Figure 3-11 and Figure 3-12 signify instances where the CoPs was exceptionally high. These can be interpreted as moments of increased postural instability, larger compensatory movements, or brief excursions of the body's CoP that deviate significantly from the typical sway pattern. The increased density and magnitude of these outliers, particularly in the CT trial, further emphasizes the heightened challenge posed by dual tasks to the participant’s balance control system. Overall, the observed consistency in CoPs patterns, including the mean, median, and spread, between the left and right foot suggests a symmetrical postural response to the various trial conditions. However, based on the CoPs outcomes, the effectiveness of the Suralis intervention remains inconclusive, as no consistent trend where median and average CoPs values were reliably higher or lower with the intervention than without was observed.

4.5 Suralis its effects on MoS

The boxplots in Figure 3-13 highlight key differences in MoS between the AP and ML directions. The consistently lower median MoS values and greater variability, evidenced by a larger interquartile range and more outliers in the AP direction, suggest that the participant faced a greater challenge in maintaining postural control in the AP plane. Conversely, the high and robust MoS in the ML direction across all trials during the first data acquisition indicates a more stable posture in the ML plane. These findings align with established understanding of balance control in individuals with lower limb amputation [1, 6].

Regarding the Suralis intervention (orange boxes), its effect on MoS was inconsistent and varied across tasks. While a slight increase in AP MoS was observed in the less demanding EO trial, this potential stabilizing benefit did not persist in more challenging tasks (EC, CT, RTT) Furthermore, no consistent benefit was observed in the ML direction. Notably, in both the EC and RTT trials, phases with the Suralis intervention even showed a reduction in AP MoS compared to their respective baseline phases. This initial data acquisition, with the participant's first use of the Suralis intervention, did not reflect a consistently beneficial outcome on MoS.

A consistent pattern during the first data acquisition across all trials was the observed learning effect, where phase A2 showed a greater MoS than phase A1, and similarly, phase B2 exhibited a greater MoS than phase B1. This suggests that the participant adapted their postural control strategies over time within each trial, likely due to repeated exposure to the task and/or the intervention, leading to improved stability. This adaptation is an aspect of motor learning in balance control, consistent with findings in the context of user adaptation to sensory feedback in prosthetic systems [10].

Finally, the presence of outliers in the boxplots, especially those extending to lower or even negative MoS values in the AP direction during challenging tasks like CT, is an important observation. These outliers represent moments of significantly reduced stability where the xCoM approaches or even momentarily falls outside the BoS, indicating a heightened risk of imbalance or the execution of large compensatory movements to prevent a fall. Their increased frequency in more challenging tasks underscores the high demands placed on the balance system, with the lack of proprioception and plantar pressure sensation likely contributing to these observations.

4.6 Limitations

This study, while providing valuable initial insights, is subject to several inherent limitations that warrant careful consideration. Primarily, the design as a single-case study inherently restricts the generalizability of our findings. The observed results are specific to the individual participant and may not be representative of a broader population with bilateral amputation. Future research would benefit from the inclusion of a larger patient cohort to establish the external validity of any observed effects and to explore potential inter-individual variability in response to the Suralis system.

Beyond the single-case design, an additional limitation was the discontinuation of the intervention during the familiarization period, which prevented the assessment of long-term adaptation or sustained effects. Our findings are therefore limited to baseline data and an initial, short-term exposure. Had the intervention been completed, it could have revealed insights into the Suralis system's long-term effects. This includes whether improvements in postural balance could be maintained or further enhanced over time. Therefore, future studies should aim for completed intervention periods with consistent participant follow-up. This will allow for a more comprehensive understanding of adaptation, sustained improvements, and the long-term feasibility of these interventions in daily life.

4.7 Contribution to the state of the art

This study presents the first specific evaluation of the IEE insole as a tool for measuring postural balance and delivering vibrotactile plantar pressure feedback through the Suralis in individuals with bilateral lower extremity amputation. While previous research, such as that by Valette et al. [12] and Kalff et al. [11], has explored the effects of vibrotactile feedback using sensor thresholds, their primary focus has been on gait performance. Our work distinctly adds to the literature by specifically focusing on static postural stability, providing a unique validation of the Suralis system for balance measurement. This advances how insole data should be used to derive balance metrics highly relevant for static tasks.

Furthermore, our findings highlight the need to refine the current mapping of sensor readings for more effective vibrotactile feedback. Instead of relying on sensor reading thresholds for vibration motor activation, our work demonstrates the potential and necessity of considering the combined output of all sensors. This approach, as evidenced by our CoP estimation with sub-10 mm RMSE, allows for an accurate and consistent feedback of plantar pressure distribution during standing. Ultimately, these findings lay a robust foundation for the future development of insole-based vibrotactile feedback systems.

5. CONCLUSION

The Suralis system, in its current state, demonstrates limitations in delivering consistent vibrotactile plantar pressure feedback. Analysis of vibration motor activation, based on predefined thresholds, revealed inconsistencies in their triggering locations. This suggests that reliance on individual sensor readings, where thresholds are not consistently met at the same physical locations, leads to unreliable feedback. Such inconsistency reduces the reliability of haptic feedback.

Despite these feedback inconsistencies, the Suralis system shows capability as a tool for measuring postural balance. Its pressure sensors exhibit a logarithmic force-response, offering sensitivity at lower pressure ranges relevant to subtle postural shifts. By integrating data from its sensors through a MLR model, the system accurately estimates the CoP, achieving a RMSE below 10 mm. This accuracy for CoP estimation indicates the Suralis its utility for assessing postural sway.

To enhance the Suralis its reliability and fulfil its potential as a feedback tool, it is advised that future development focuses on optimizing vibrotactile activation strategies by employing multi-sensor algorithms, rather than relying solely on individual sensor thresholds. Further study is required to determine the appropriate weights and thresholds for such combined sensor output to achieve consistent and meaningful feedback.

Regarding the intervention's effects, the limited baseline data from a single participant does not allow us to conclude an effect of the Suralis on postural balance. Therefore, further study with an intervention period and effect measurement is required to systematically evaluate its impact on objective balance metrics.

REFERENCES

[1] L. Chen, Y. Feng, B. Chen, Q. Wang, and K. Wei, "Improving postural stability among people with lower-limb amputations by tactile sensory substitution," *J Neuroeng Rehabil,* vol. 18, no. 1, p. 159, Nov 6 2021, doi: 10.1186/s12984-021-00952-x.

[2] S. K. Dhillon, S. Venkataraman, A. R. Chanu, G. Handa, and S. Wadhwa, "A cross-sectional study to assess dual-task interference in postural control in people with lower limb amputation," *Gait Posture,* vol. 113, pp. 204-208, Jun 20 2024, doi: 10.1016/j.gaitpost.2024.06.013.

[3] S. R. Koehler-McNicholas, B. C. Savvas Slater, K. Koester, E. A. Nickel, J. E. Ferguson, and A. H. Hansen, "Bimodal ankle-foot prosthesis for enhanced standing stability," *PLoS One,* vol. 13, no. 9, p. e0204512, 2018, doi: 10.1371/journal.pone.0204512.

[4] A. C. Nanivadekar *et al.*, "SPINAL CORD STIMULATION RESTORES SENSATION, IMPROVES FUNCTION, AND REDUCES PHANTOM PAIN AFTER TRANSTIBIAL AMPUTATION," 2022, doi: 10.1101/2022.09.15.22279956.

[5] B. A. Petersen, P. J. Sparto, and L. E. Fisher, "Clinical measures of balance and gait cannot differentiate somatosensory impairments in people with lower-limb amputation," *Gait Posture,* vol. 99, pp. 104-110, Jan 2023, doi: 10.1016/j.gaitpost.2022.10.018.

[6] P. X. Ku, N. A. Abu Osman, and W. A. Wan Abas, "Balance control in lower extremity amputees during quiet standing: a systematic review," *Gait Posture,* vol. 39, no. 2, pp. 672-82, 2014, doi: 10.1016/j.gaitpost.2013.07.006.

[7] M. R. Prins, N. Kluft, W. Philippart, H. Houdijk, J. H. van Dieën, and S. M. Bruijn, "Limitation of Ankle Mobility Challenges Gait Stability While Walking on Lateral Inclines," presented at the Wearable Robotics: Challenges and Trends, 2022, Chapter 100, doi: 10.1007/978-3-030-69547-7_100.

[8] S. Ettema, E. Kal, and H. Houdijk, "General estimates of the energy cost of walking in people with different levels and causes of lower-limb amputation: a systematic review and meta-analysis," *Prosthet Orthot Int,* vol. 45, no. 5, pp. 417-427, Oct 1 2021, doi: 10.1097/PXR.0000000000000035.

[9] E. C. Wentink, A. Mulder, J. S. Rietman, and P. H. Veltink, "Vibrotactile stimulation of the upper leg: effects of location, stimulation method and habituation," *Annu Int Conf IEEE Eng Med Biol Soc,* vol. 2011, pp. 1668-71, 2011, doi: 10.1109/IEMBS.2011.6090480.

[10] E. C. Wentink, "Feasibility of enhanced user control and feedback in upper leg prostheses," Biomedical Signals and Systems, Faculty of Electrical Engineering, Mathematics and Computer Science (EEMCS), University of Twente, 2013, doi: 10.3990/1.9789036511957.

[11] M. N. Kalff *et al.*, "Impact of Gait-Synchronized Vibrotactile Sensory Feedback on Gait in Lower Limb Amputees," *Applied Sciences,* vol. 14, no. 23, 2024, doi: 10.3390/app142311247.

[12] R. Valette, S. Manz, J. Gonzalez-Vargas, and S. Dosen, "Intuitive omnidirectional vibrotactile feedback from a sensorized insole for lower-limb prostheses users: a preliminary assessment," *J Neural Eng,* Jun 10 2025, doi: 10.1088/1741-2552/ade343.

[13] A. M. Aries, P. Downing, J. Sim, and S. M. Hunter, "Effectiveness of Somatosensory Stimulation for the Lower Limb and Foot to Improve Balance and Gait after Stroke: A Systematic Review," *Brain Sci,* vol. 12, no. 8, Aug 19 2022, doi: 10.3390/brainsci12081102.

[14] B. C. Eapen, D. P. Murphy, and D. X. Cifu, "Neuroprosthetics in amputee and brain injury rehabilitation," *Exp Neurol,* vol. 287, no. Pt 4, pp. 479-485, Jan 2017, doi: 10.1016/j.expneurol.2016.08.004.

[15] T. J. Arakeri, B. A. Hasse, and A. J. Fuglevand, "Object discrimination using electrotactile feedback," *J Neural Eng,* vol. 15, no. 4, p. 046007, Aug 2018, doi: 10.1088/1741-2552/aabc9a.

[16] J. Gonzalez-Vargas, M. Sartori, S. Dosen, H. van der Kooij, and J. Rietman, "SimBionics: Neuromechanical Simulation and Sensory Feedback for the Control of Bionic Legs," in *Wearable Robotics: Challenges and Trends*, Cham, J. C. Moreno, J. Masood, U. Schneider, C. Maufroy, and J. L. Pons, Eds., 2022: Springer International Publishing, 2022, pp. 269-273, doi: 10.1007/978-3-030-69547-7_44.

[17] R. Valette, J. Gonzalez-Vargas, and S. Dosen, "The impact of walking on the perception of multichannel electrotactile stimulation in individuals with lower-limb amputation and able-bodied participants," *J Neuroeng Rehabil,* vol. 20, no. 1, p. 108, Aug 17 2023, doi: 10.1186/s12984-023-01234-4.
[18] B. P. Christie, H. Charkhkar, C. E. Shell, C. J. Burant, D. J. Tyler, and R. J. Triolo, "Ambulatory searching task reveals importance of somatosensation for lower-limb amputees," *Sci Rep,* vol. 10, no. 1, p. 10216, Jun 23 2020, doi: 10.1038/s41598-020-67032-3.
[19] IEE, "8 cell insole Datasheet v04," 21-12-16 2016.
[20] "Lower body modeling with Plug-in Gait." Vicon Motion Systems. [Online]. Available: https://help.vicon.com/space/Nexus216/11605140/Lower+body+modeling+with+Plug-in+Gait (accessed Apr. 8, 2025).
[21] L. E. Powell and A. M. Myers, "The Activities-specific Balance Confidence (ABC) Scale," *J Gerontol A Biol Sci Med Sci,* vol. 50A, no. 1, pp. M28-34, Jan 1995, doi: 10.1093/gerona/50a.1.m28.
[22] K. Berg, "Measuring balance in the elderly: preliminary development of an instrument," *Physiotherapy Canada,* vol. 41, no. 6, pp. 304-311, 1989, doi: 10.3138/ptc.41.6.304.
[23] A. Krasny-Pacini and J. Evans, "Single-case experimental designs to assess intervention effectiveness in rehabilitation: A practical guide," *Ann Phys Rehabil Med,* vol. 61, no. 3, pp. 164-179, May 2018, doi: 10.1016/j.rehab.2017.12.002.
[24] S. J. Morgan, B. J. Hafner, D. Kartin, and V. E. Kelly, "Dual-task standing and walking in people with lower limb amputation: A structured review," *Prosthet Orthot Int,* vol. 42, no. 6, pp. 652-666, Dec 2018, doi: 10.1177/0309364618785728.
[25] A. L. Hof, "The 'extrapolated center of mass' concept suggests a simple control of balance in walking," *Hum Mov Sci,* vol. 27, no. 1, pp. 112-25, Feb 2008, doi: 10.1016/j.humov.2007.08.003.
[26] A. L. Hof, "The equations of motion for a standing human reveal three mechanisms for balance," *J Biomech,* vol. 40, no. 2, pp. 451-7, 2007, doi: 10.1016/j.jbiomech.2005.12.016.
[27] V. M. Santos, B. B. Gomes, M. A. Neto, and A. M. Amaro, "A Systematic Review of Insole Sensor Technology: Recent Studies and Future Directions," *Applied Sciences,* vol. 14, no. 14, 2024, doi: 10.3390/app14146085.
[28] W. Kilian, M. Hill, and S. Odenwald, "Adaptive Sensor Data Acquisition for Gait Analysis," *Procedia Engineering,* vol. 147, pp. 659-664, 2016, doi: 10.1016/j.proeng.2016.06.267.
[29] P. Jamali, L. S. Chou, and R. D. Catena, "Whole-cycle and time-specific validation of a GUI-based ground reaction force estimation tool for clinical gait analysis without a force plate," *Med Eng Phys,* vol. 141, p. 104366, Jul 2025, doi: 10.1016/j.medengphy.2025.104366.

APPENDIX A AI STATEMENT

During the preparation of this work the author used Gemini in order to generate initial outlines for sections and refine the overall language and readability. After using this tool/service, the author reviewed and edited the content as needed and takes full responsibility for the content of the work. Additionally, Gemini's coding partner was used for debugging Python code employed in both the analysis and visualisation of the data, with all suggested corrections reviewed and validated by the author.

APPENDIX B BASELINE CONTEXTUAL MEASURES

A questionnaire for demographic data, the BBS [22], and the ABC scale [21] served as baseline contextual measures. Their outcomes are reported in Table B.1, Table B.2, and Table B.3 respectively.

Table B.1: Participant demographics.

Sex	Male
Age	54 years
Length (self-reported)	192 cm
Weight (self-reported)	90 kg
Level of amputation, left	Transtibial
Level of amputation, right	Transtibial
Time since amputation, left	21 years
Time since amputation, right	12 years
Cause of amputation, left	Vasculair (Thromboangiitis obliterans)
Cause of amputation, right	Vasculair (Thromboangiitis obliterans)
Current prosthesis, left	BAP: GV20 connector with tales side-flex size 26
Current prosthesis, right	BAP: GV20 connector with tales side-flex size 26
Stump length, left	11.5 cm from knee joint line to the point perpendicular to the stump at its most distal aspect.
Stump length, right	14.5 cm from knee joint line to the point perpendicular to the stump at its most distal aspect.
Prosthesis use	15 hours per day
K-level	K4 (Outdoor walker with particularly high demands, very active adult)

Table B.2: BBS results.

Tasknumber	*Task*	Score
1	*Sit to stand*	4 / 4
2	*Standing independently*	4 / 4
3	*Sitting independently*	4 / 4
4	*From stance to sit*	4 / 4
5	*Transfers*	4 / 4
6	*Standing with eyes closed*	4 / 4
7	*Standing independently with the feet together*	4 / 4
8	*Reaching forward with stretched arm in stance*	3 / 4
9	*Picking up an object from the floor from stance*	4 / 4
10	*Turning to look over the left and right shoulder to look back while standing*	2 / 4
11	*Make a 360° turn in stance*	4 / 4
12	*Alternatingly place feet on step in stance*	4 / 4
13	*Standing in tandem stance*	0 / 4
14	*Standing on one leg*	1 / 4
Total score		46 / 56

Table B.3: ABC scale results. For each task, the question was: How confident are you that you will not fall or lose your balance when you are...

Tasknumber	*Task*	Score
1	*walking through the house*	95%
2	*walking stairs up or down*	95%
3	*bending over to pick up a slipper lying at the front of a cupboard*	70%
4	*reaching for a can of tea that is on a shelf at eye level?*	95%
5	*standing on your toes and reaching for something above your head?*	70
6	*standing on a chair and reaching for something*	70%
7	*sweeping the floor*	95%
8	*walking outside the house to a car parked in the driveway*	100%
9	*getting in or out of the car*	100%
10	*walking across a car park to a shopping centre*	90%
11	*walking up or down a slope*	90%
12	*walking in a busy shopping centre people pass you by quickly*	90%
13	*walking in a busy shopping centre and people bumping into you*	90%
14	*stepping onto or off the escalator with your hands on the handrail*	100%
15	*stepping onto or off the escalator with shoppingbags in your hands, which prevents you from holding onto the handrail.*	90%
16	*walking on a pavement covered with snow or ice*	50%

APPENDIX C SURALIS SETTINGS AFTER CALIBRATION

The vibration motors were calibrated such that the participant perceived each motor with the same intensity. Furthermore, vibration motor activation thresholds were set, such that when the subject leans anteriorly or posteriorly, the corresponding vibration motor activates. Regarding medial and lateral directions, a shift in weight from one leg to the other was perceived well, although feeling for a single leg at the initial fitting was complicated for the participant. The threshold for activation of the metatarsal bone vibration motors was kept at factory settings, which is below the values measured in stance. This resulted in the metatarsal vibration motors activating only when placing the feet down, not when leaning from a stance position.

Table C.1: Suralis settings after calibration.

Setting	*Left*	*Right*
Threshold heel	63%	69%
Threshold fifth metatarsal bone	30%	30%
Threshold first metatarsal bone	30%	30%
Threshold hallux + toes	64%	45%
Vibration intensity heel	55%	40%
Vibration intensity fifth metatarsal bone	55%	40%
Vibration intensity first metatarsal bone	70%	45%
Vibration intensity hallux + toes	55%	40%

For both systems, the vibration duration was set to 2.54 seconds for the heel and hallux + toes vibration motors.

APPENDIX D SYNCHRONISED SIGNALS

Synchronised signals of the force measured by the GRAIL (blue) and the pressure measured by the Suralis (red) per phase.

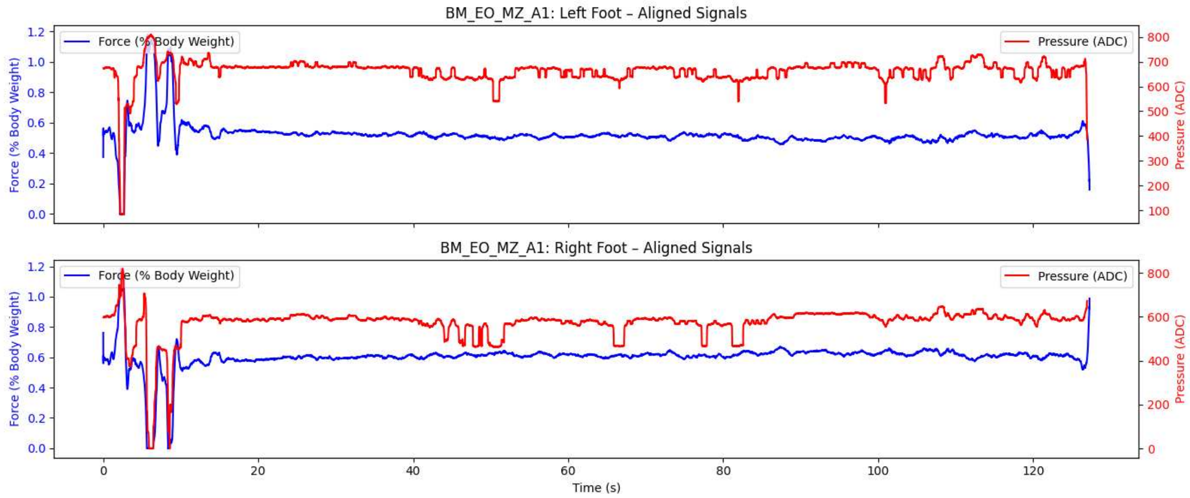

Figure D-1: Trial EO, Phase A1. Force signal (GRAIL) synchronised with total raw pressure output (Suralis).

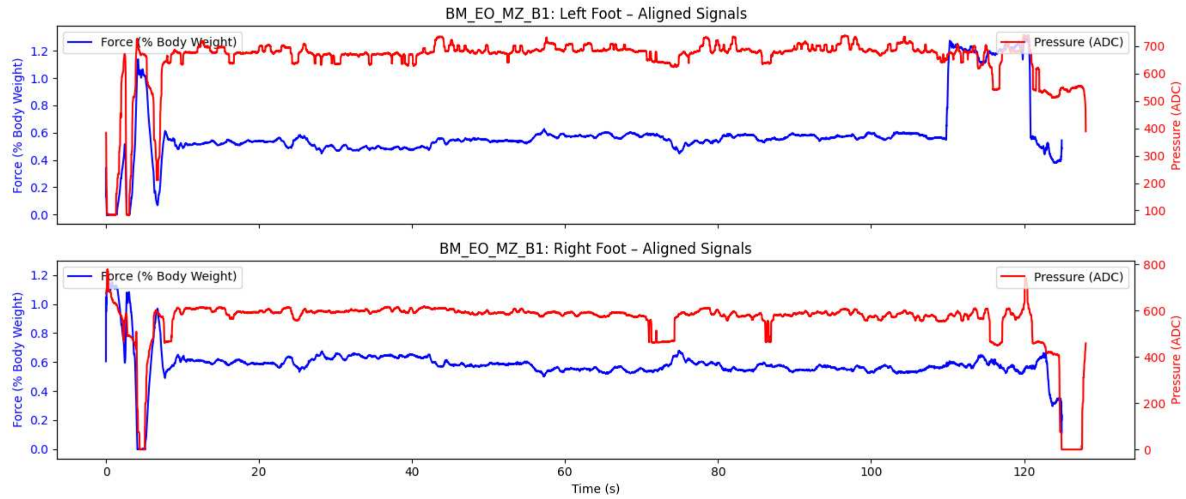

Figure D-2: Trial EO, Phase B1. Force signal (GRAIL) synchronised with total raw pressure output (Suralis).

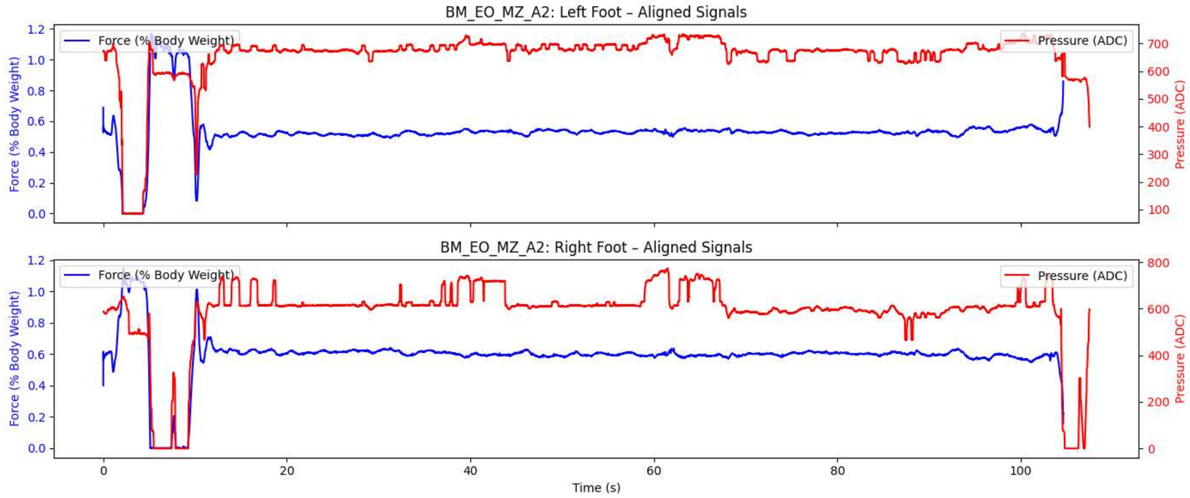

Figure D-3: Trial EO, Phase A2. Force signal (GRAIL) synchronised with total raw pressure output (Suralis).

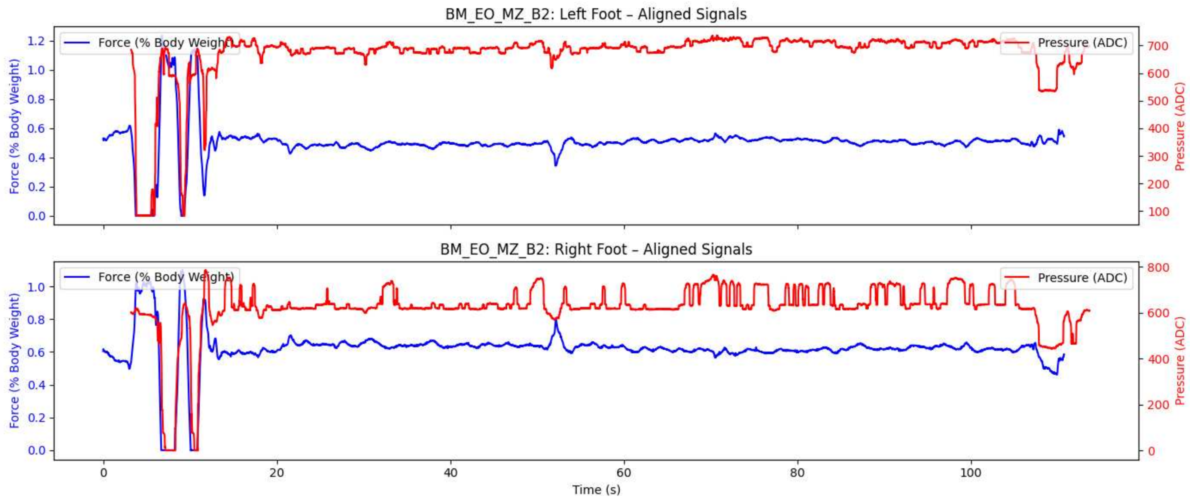

Figure D-4: Trial EO, Phase B2. Force signal (GRAIL) synchronised with total raw pressure output (Suralis).

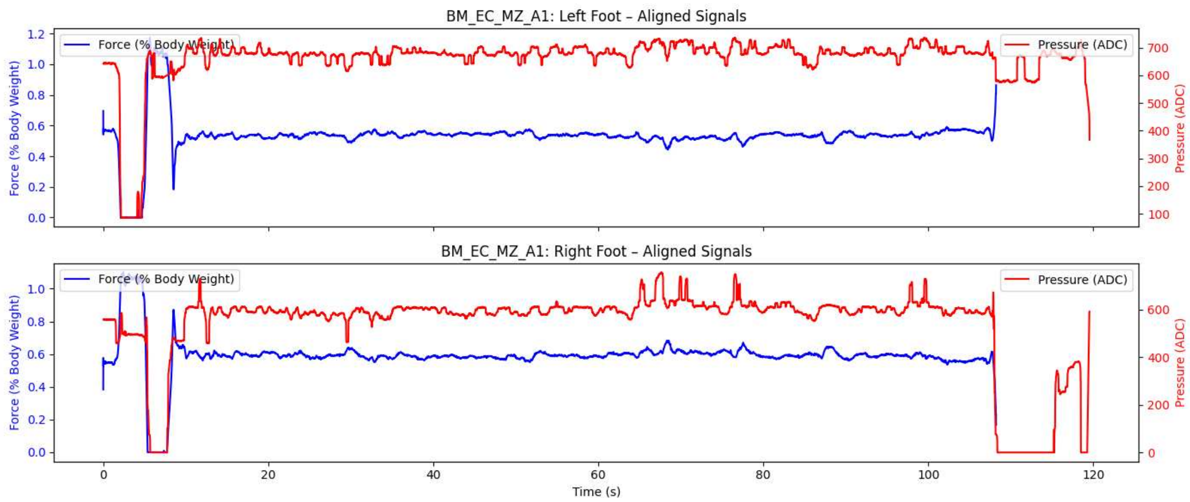

Figure D-5: Trial EC, Phase A1. Force signal (GRAIL) synchronised with total raw pressure output (Suralis).

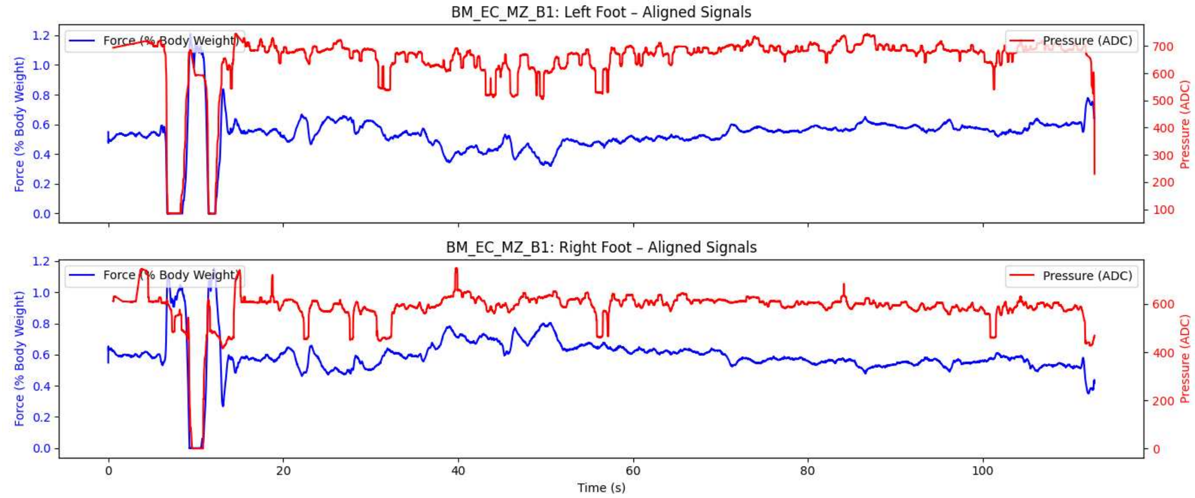

Figure D-6: Trial EC, Phase B1. Force signal (GRAIL) synchronised with total raw pressure output (Suralis).

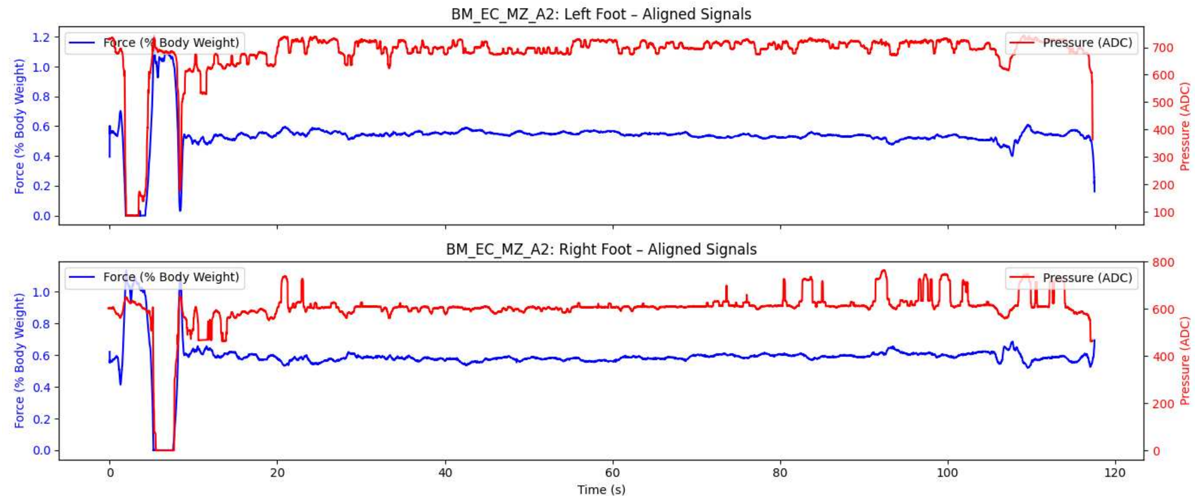

Figure D-7: Trial EC, Phase A2. Force signal (GRAIL) synchronised with total raw pressure output (Suralis).

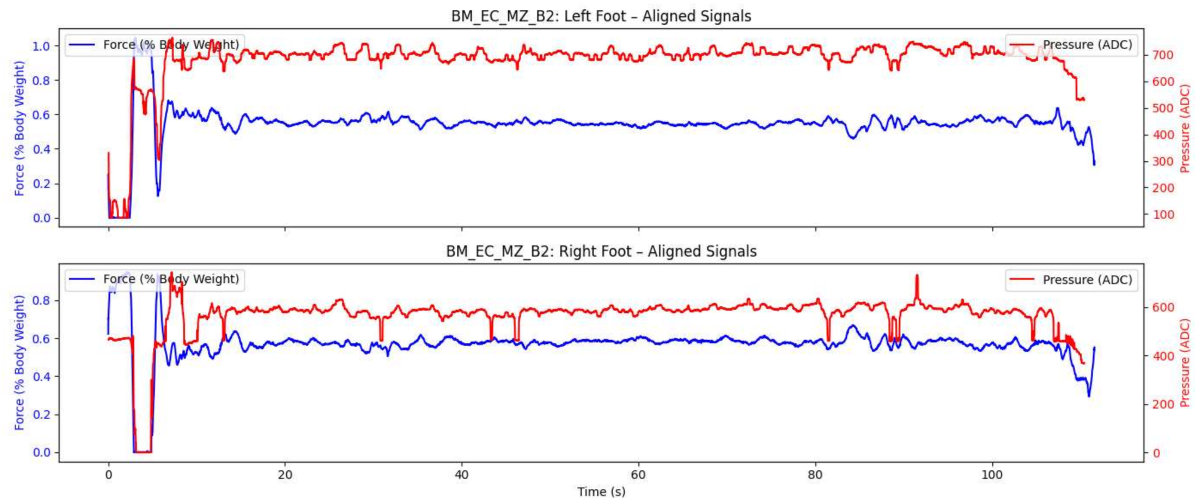

Figure D-8: Trial EC, Phase B2. Force signal (GRAIL) synchronised with total raw pressure output (Suralis).

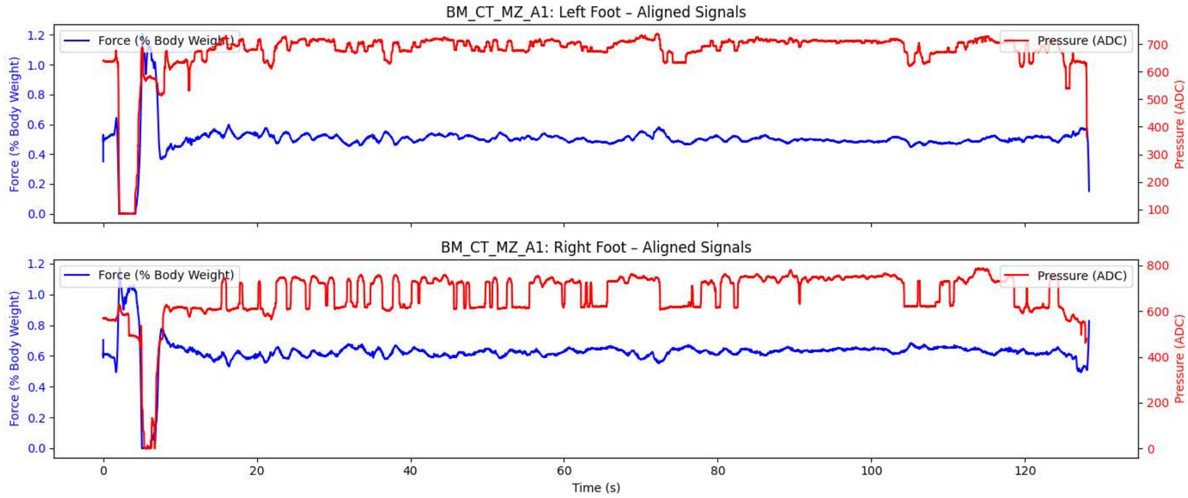

Figure D-9: Trial CT, Phase A1. Force signal (GRAIL) synchronised with total raw pressure output (Suralis).

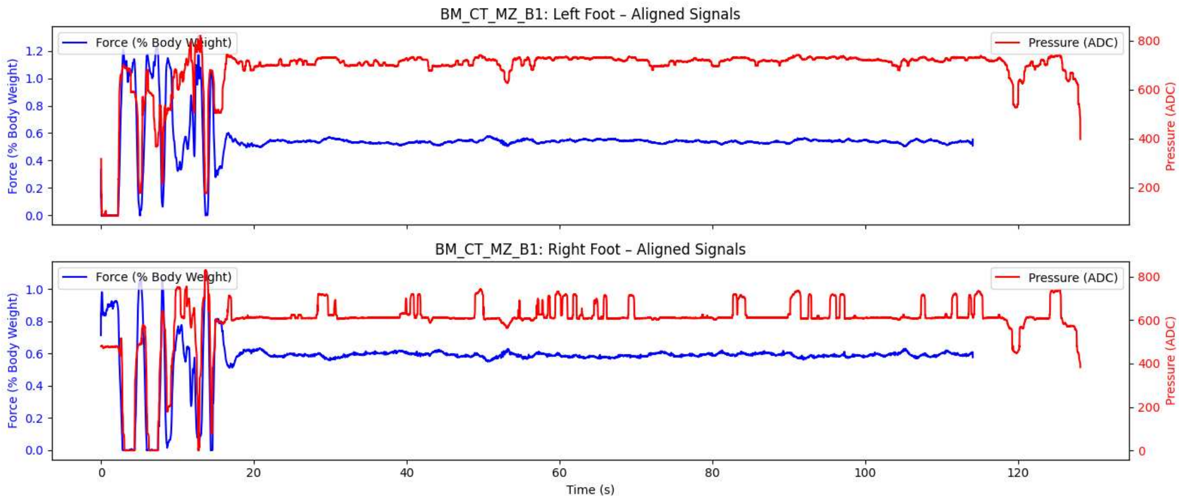

Figure D-10: Trial EC, Phase B1. Force signal (GRAIL) synchronised with total raw pressure output (Suralis).

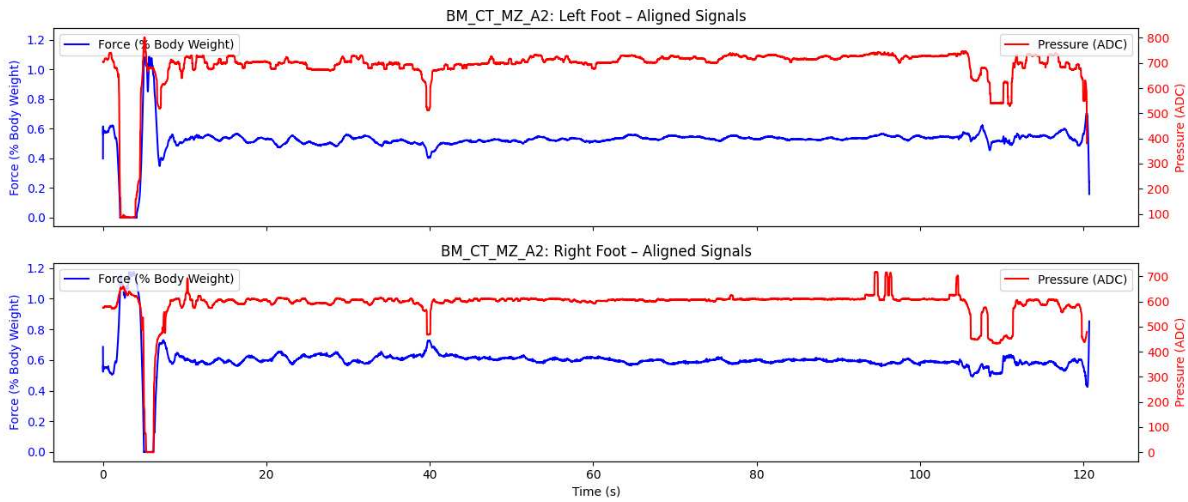

Figure D-11: Trial CT, Phase A2. Force signal (GRAIL) synchronised with total raw pressure output (Suralis).

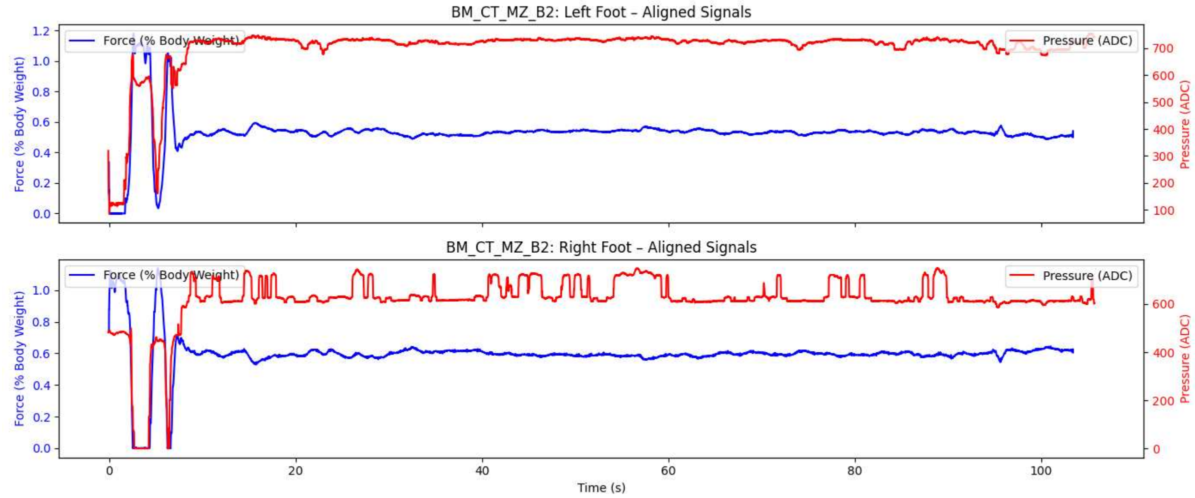

Figure D-12: Trial CT, Phase B2. Force signal (GRAIL) synchronised with total raw pressure output (Suralis).

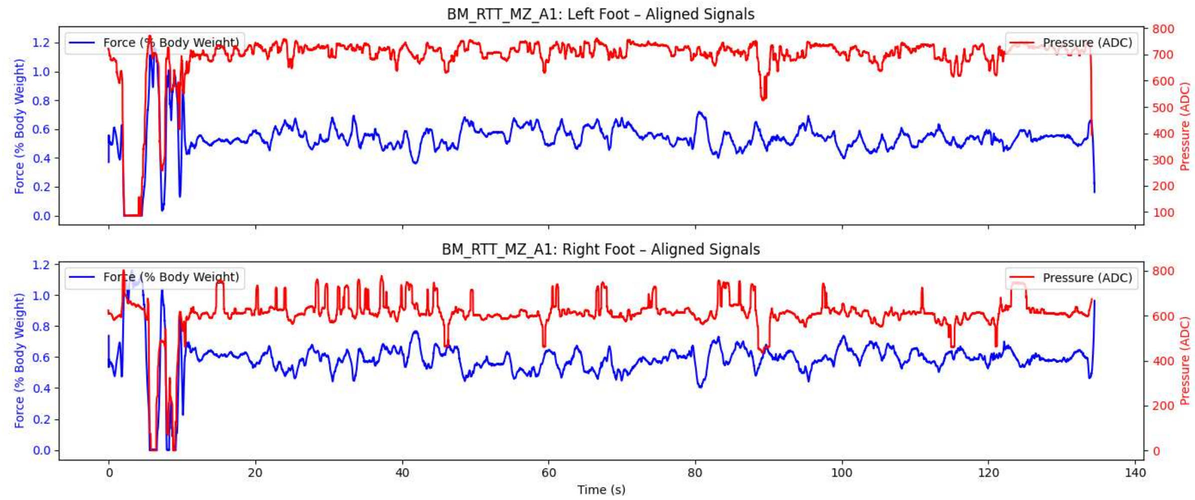

Figure D-13: Trial RTT, Phase A1. Force signal (GRAIL) synchronised with total raw pressure output (Suralis).

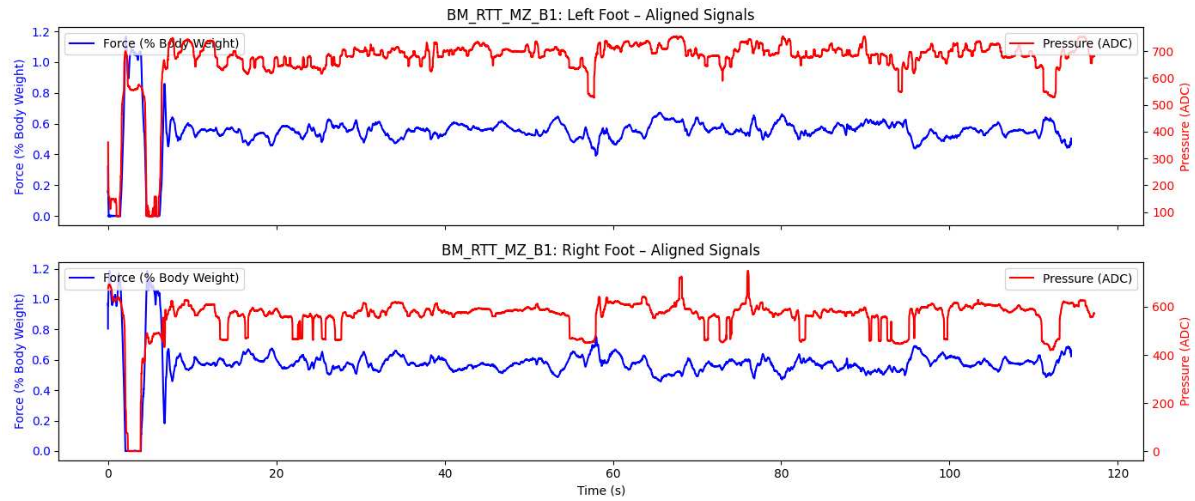

Figure D-14: Trial RTT, Phase B1. Force signal (GRAIL) synchronised with total raw pressure output (Suralis).

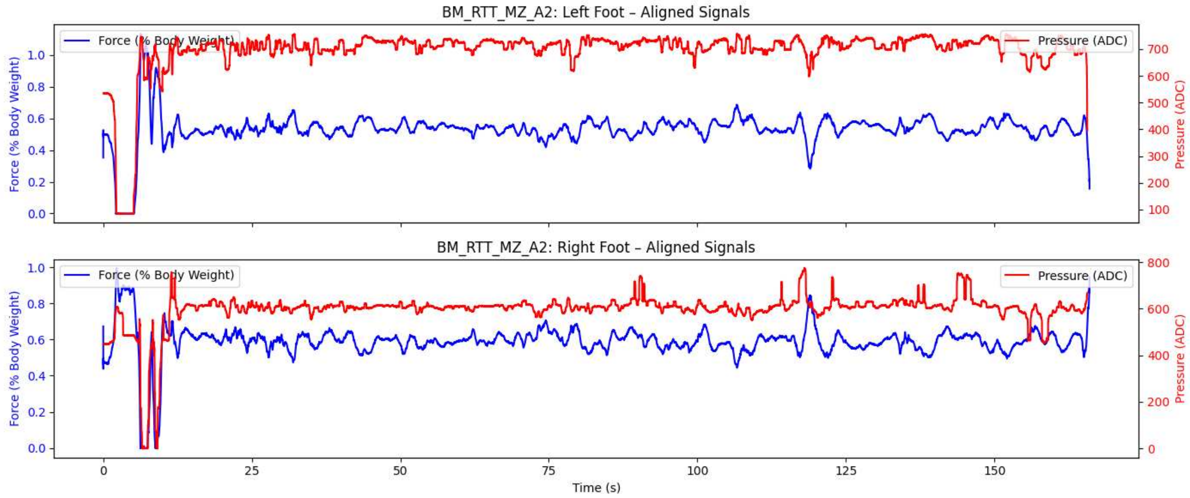

Figure D-15: Trial RTT, Phase A2. Force signal (GRAIL) synchronised with total raw pressure output (Suralis).

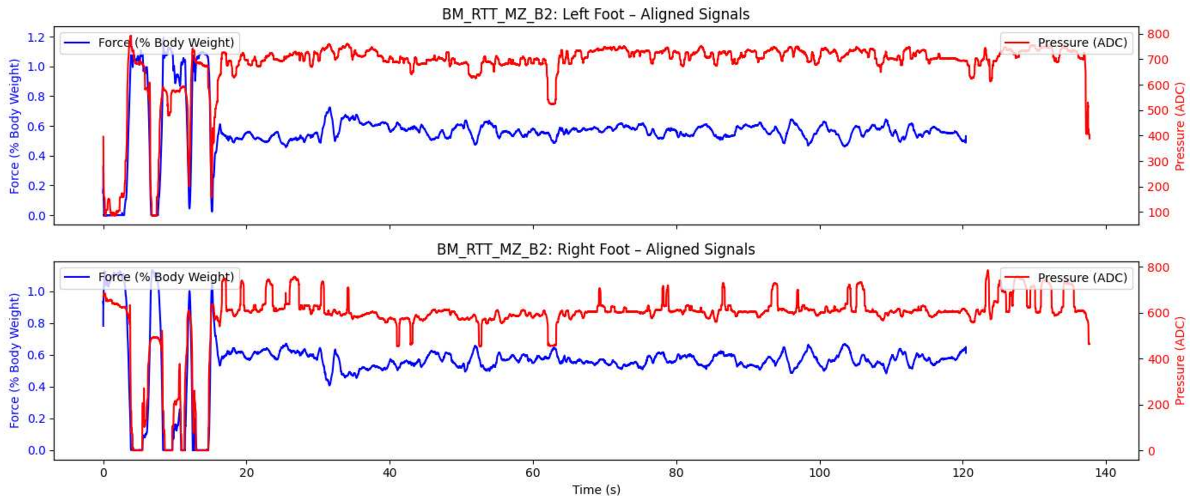

Figure D-16: Trial RTT, Phase B2. Force signal (GRAIL) synchronised with total raw pressure output (Suralis).

APPENDIX E COP LOCATIONS FOR THE FIRST AND FIFTH METATARSAL

Figures of the CoP locations measured by the GRAIL during the first data acquisition across all trials coloured by the raw pressure sensor output of the first and fifth metatarsal sensors.

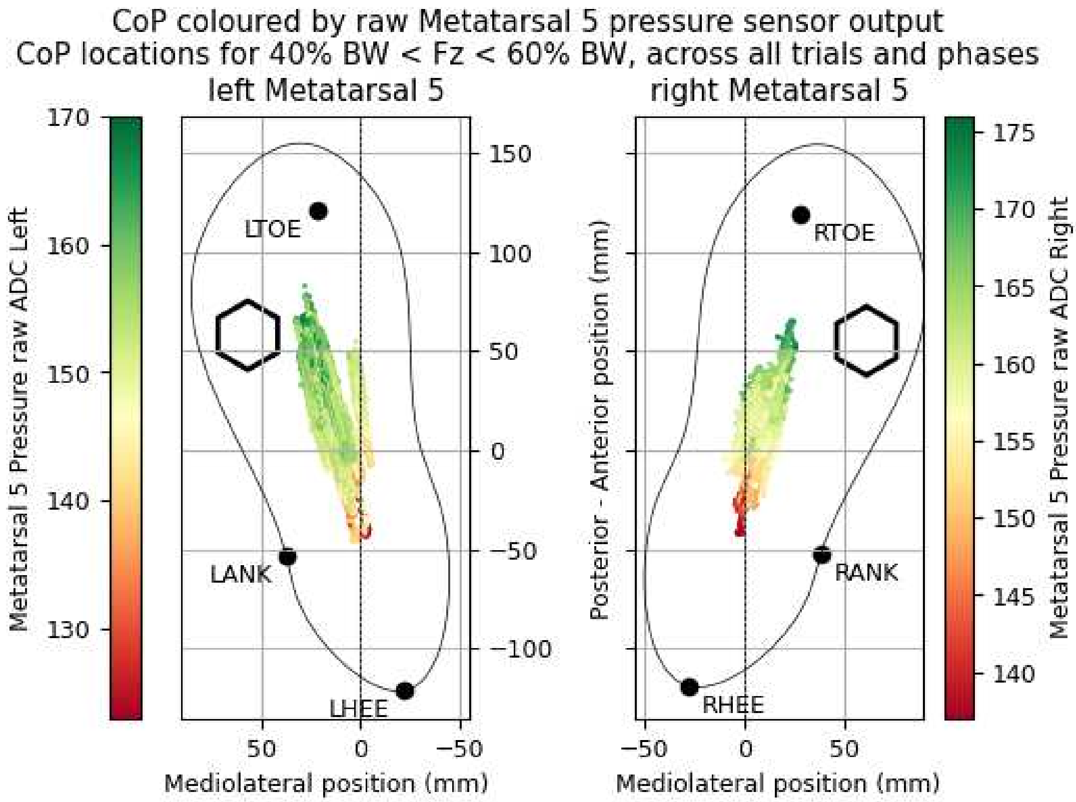

Figure E-1: CoP coloured by the raw fifth metatarsal pressure sensor output during the first data acquisition, across all four trials and phases.

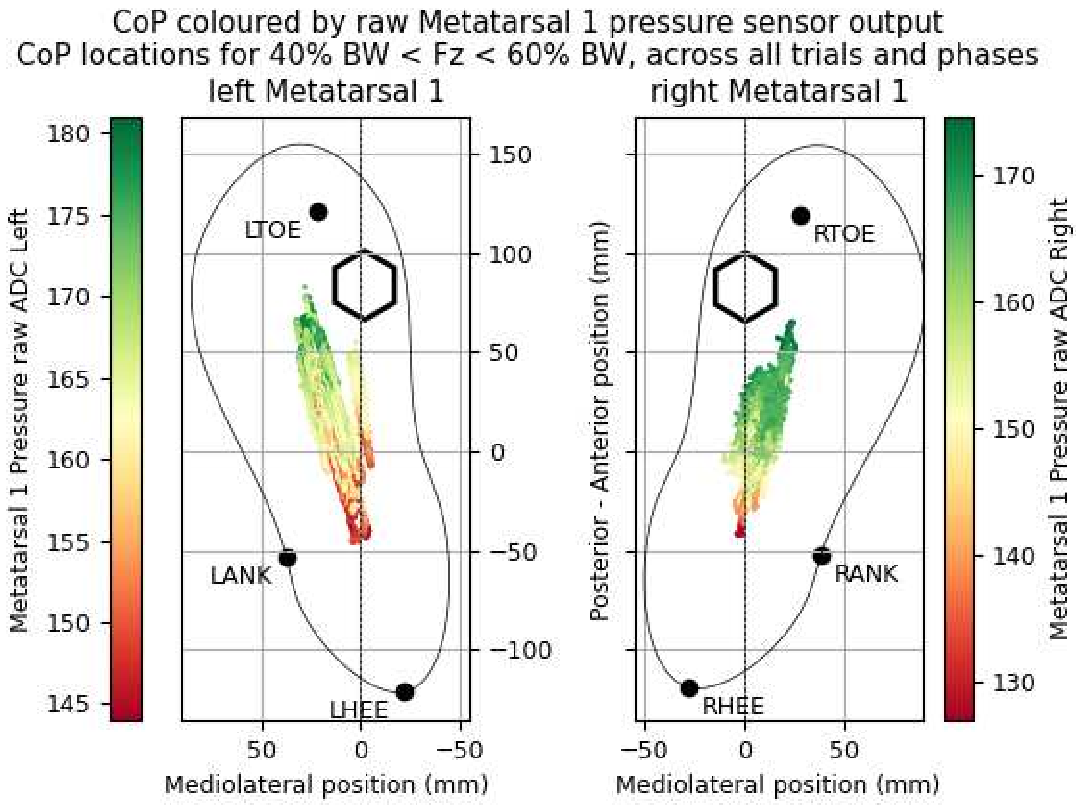

Figure E-2: CoP coloured by the raw first metatarsal pressure sensor output during the first data acquisition, across all four trials and phases.

APPENDIX F RESULTS OF THE COGNITIVE TASK AND REACH AND TARGET TASK

This appendix presents the results obtained during the baseline data acquisition for trial CT and RTT. Table F.1 presents the percentage of correct answers from the Stroop tests performed during each phase of the CT trial. We observed that the score increased with each phase.

Table F.1: Results of the strooptest.

Phase	*Score*
A1	72%
B1	85%
A2	96%
B2	97%

Table F.2 presents the results of the kite flyer application. The goal was to collect tokens and to dodge other kites. The results for phases A1, A2, and B2 show that 26 tokens were collected and 0 collisions occurred. However, during phase B1, 26 tokens were collected and 2 collisions occurred.

Table F.2: Results of the Reach and Target Task.

Phase	*Tokens collected*	*Collisions*
A1	26	0
B1	25	2
A2	26	0
B2	26	0